Spring 2024

Managing Stress: A Study of Stress Response Mechanisms in Mycobacteria

Augusto C. Hunt Serracin
University of Texas at Arlington

Managing Stress: A Study of Stress Response Mechanisms in Mycobacteria

by

Augusto César Hunt Serracín

DISSERTATION

Submitted in partial fulfillment of the requirements
for the degree of Doctor of Philosophy

The University of Texas at Arlington

May 2024

Supervising Committee:

Dr. Cara C. Boutte, Advisor and Committee Chair

Dr. Joseph M. Boll, Committee Member

Dr. Mark W. Pellegrino, Committee Member

Dr. Melissa J. Walsh, Committee Member

Dr. Todd A. Castoe, Committee Member

Acknowledgements

First, this journey has been a humbling and growing experience for me as an individual and professional. I thank God for this season of my life, during which I was able to meet some incredible people and add new cast members to the story that makes up my life. I want to thank the love of my life, my wife Tania, for all these years of endless support and encouragement. Thank you for all your hard work and for keeping a roof over our heads. I also thank my little mini-me, my daughter, Amelia. Thank you for loving me unconditionally and for the many sweet hugs at the end of every workday.

To my advisor and mentor, Cara Boutte, thank you for your guidance, patience, and support throughout my graduate school career. It was a pleasure and honor to help you start the lab almost seven years ago. I look forward to witnessing all the fantastic research that will come out of the Boutte lab. Thank you, Cara, for hiring me as an assistant with little research experience and giving me this life-changing opportunity. Thank you for always encouraging me to become a better thinker. I am going to miss my yearly bottle of maple syrup, as well as washing my hands with homemade lemongrass soap. (And Sunny! I will miss Sunny too)

To my graduate committee, Dr. Boll, Dr. Walsh, Dr. Castoe, Dr. Pellegrino, I extend my sincere gratitude to you for your time, expertise, guidance, and support throughout this academic journey. Your feedback and encouragement have been instrumental in shaping me as a person and researcher. I am truly grateful for your commitment to my success. Thank you for choosing to be part of my story.

To all current and former members of the Boutte lab, thank you for being a family away from home. I am excited to see where life takes every single one of you. Thank you for hours of

brainstorming, emotional support, and fellowship. To Dr. Farah Shamma, thank you for making my transition into academic research a little less scary. Thank you for being my sounding board through the good and challenging moments. Thank you for helping me do the math. To Neda Habibi, MD, and now PhD, we made it, Neda! Thank you for being such an organized and knowledgeable human being. Thank you for always answering my "quick" questions. Thank you for always taking time to talk about results and helping me troubleshoot experiments. To Dr. Angela Freeman, my former desk neighbor, thank you for always lending an ear and sharing your food with me. Thank you for the advice, help, and all the resources you shared that helped me pass my classes. To Anusuya Nepal and Karen Tembiwa, thank you for all your help, support, and many laughs in these last couple of years of the program. I look forward to seeing you both grow and lead the next group of Boutte lab graduate students. To my two "undergraduate" students, Brian Parks, and Arinze Awagu, thank you for your time and efforts. It was a joy to teach you the little that I knew, but more than anything, it was a pleasure to work together. Thank you both for keeping me honest and helping me complete my projects; I will forever be indebted. To lab members in the current and past quad lab, thank you for being excellent colleagues. Thank you for sharing your knowledge and expertise and always taking the time to talk science. To Dr. Soroush Ghaffari, thank you for always being a solid resource when science got tough. Thank you for your time and willingness to share your scientific knowledge.

Finally, I want to express my deepest gratitude to my parents. To my mom, your sacrifices and encouragement in my early life have shaped me into the professional I am today. To my dad, your encouragement to always ask questions and seek answers has fostered my sense of wonder. Thank you, Mom, and Dad, for equipping me with the tools to navigate life and become the man I am today.

Table of Contents

ABSTRACT

Mycobacteria encompass many pathogenic species known to cause severe disease in humans. A well-known example is *Mycobacterium tuberculosis* (*Mtb*), the causative agent of the lung disease tuberculosis, which kills millions of humans worldwide yearly. Pathogenic mycobacteria like *Mtb* are challenging to treat because of their innate ability to adapt to environmental stress. Their unique cell physiology and conserved stress responses allow them to combat biological insults, regulate growth, and regulate genes involved in stress; all these responses increase tolerance to antibiotics. The current therapies to treat mycobacterial infections are lengthy and, at times, unsuccessful, partly due to antibiotic tolerance. A better understanding of mycobacteria cell physiology and stress response will promote the development of better treatments for chronic and recurring antibiotic-tolerant infections. Here, our work focuses on three important aspects of mycobacterial cell biology often associated with survival and antibiotic tolerance: the stringent response (a conserved stress response in bacteria), biofilm formation, and cell wall regulation.

We used *Mycobacterium abscessus* (*Mab*), a pathogen that causes soft tissue and respiratory infections, for stringent response and biofilm studies. We found that media composition affects the structure and composition of *Mab* biofilms, and the susceptibility of planktonic cells to antibiotics. In addition, we also discovered that *Mab's* stringent response pathway uses a non-canonical alarmone synthesis pathway. To study cell wall regulation, we used *Mycobacterium smegmatis*, a fast-growing non-pathogenic species commonly used to study the Mycobacterium genus. We focused on investigating the relationship between two essential growth proteins, CwlM and MurA, which are involved in the metabolism of the peptidoglycan layer, the primary layer in mycobacteria that provides shape and rigidity. We found that the

interaction between MurA (the enzyme) and CwlM (its regulator) is transient. We also identified the likely interaction site between CwlM and MurA, which affects the production of precursors by MurA. In addition, we investigated the survival and cell physiology of interaction site mutants, which shed light into understanding the role of CwlM's regulation of MurA during mycobacterial growth.

Chapter 1 - Introduction

1.1 General overview of pathogenic mycobacteria

Historically, pathogenic mycobacteria have remained a constant burden to humankind. The most well-known mycobacterial pathogens are *Mycobacterium tuberculosis* (*Mtb*), the causative agent of the respiratory disease tuberculosis (TB), and *Mycobacterium leprae*, the causative agent of leprosy. Today, *Mtb* affects millions of people worldwide, with about 10 million people contracting Tuberculosis and about 1.5 million dying from the disease. Most cases come from Pakistan, Bangladesh, Indonesia, the Philippines, China, Nigeria, and South Africa[1]. In contrast, the majority of leprosy cases are in South American, Asian, and African countries, with most cases found in Brazil, India, and Indonesia[2]. Leprosy has been better controlled due to better hygienic conditions and practices, early detection, and efficient treatments.

Non-tuberculous mycobacteria (NTM) are another category of pathogenic mycobacteria. These are opportunistic mycobacterial pathogens that do not cause TB but can still cause respiratory disease and severe soft-tissue infections. Examples of notable NTMs are *Mycobacterium avium*, originally described as causing "tuberculosis" in chickens; M*ycobacterium bovis*, a species that causes respiratory disease in cattle and humans; and *Mycobacterium abscessus*, a species known to cause multi-organ infections, lung disease, skin, and blood infections[3]. Research suggests that infections are more common in immunosuppressed individuals or those with underlying diseases, likely due to individuals encountering contaminated surfaces and water sources, such as through home materials that promote biofilm formation[4].

Even with today's modern medicine, pathogenic mycobacteria continue to impose severe challenges on the healthcare system. Mycobacteria like *Mtb* and NTMs are highly antibiotic-

resistant, making them difficult to treat. Current therapies are lengthy and require a combination of antibiotics that often include adverse side effects[5], which leads to another obstacle in treatment: poor patient compliance.

1.2 *Mycobacterium tuberculosis* and TB

1.2.1 History and current treatment: It has been well over a century since the article "The Etiology of Tuberculosis" was published in 1882. There, scientist Robert Koch made his discovery on the causative agent of TB, a tubercle bacillus he isolated, now called *Mycobacterium tuberculosis*. Koch's studies on *Mtb* were geared towards one day finding a cure for TB, and deliver humankind from this dreadful disease[6]. Since then, scientists have made significant advancements in prevention, diagnosis, and treatment to help decrease tuberculosis mortality and morbidity. Unfortunately, today, we continue to battle this persistent and dangerous bacterium.

According to the World Health Organization, TB continues to be a significant threat to human health for individuals all around the globe. The current first-line treatment is known as the RIPE TB treatment, which involves a combination of several drugs: **R**ifampin, **I**soniazid, **P**yrazinamide, and **E**thambutol[7]. These drugs serve specific purposes depending on their mechanism of action, but all of these come with adverse effects, such as severe liver toxicity. This first line of antibiotics inhibits bacterial DNA replication/transcription processes and targets cell wall synthesis[8]. If these drugs are not efficient, physicians can use the second line of antibiotics, which tend to be more efficient but also come with more severe side

effects. The second line of mycobacterial drugs consists of aminoglycosides and fluoroquinolones, which affect protein and DNA synthesis, respectively.

These drug regimens demand full patient compliance and can take several months to a year, depending on the patient's background and disease progression[9]. Unfortunately, individuals who begin to feel better or feel exhausted by the drug regimen tend to stop their treatment prematurely. Stopping the treatment not only causes individuals to become ill again but also encourages the bacteria to become drug-resistant. Although physicians can use different kinds of antibiotics, improper therapy plans can also enhance *Mtb's* ability to become multi-drug resistant (MDR). The current approach for detecting MDR-*Mtb* is to identify which drug the bacterium is resistant to, followed by identifying which drug the bacterium is sensitive to. The current line of drugs for MDR consists of Bedaquiline, the pro-drug Delamanid, Linezolid, and Pretomanid. Which inhibit *Mtb*'s energy supply, cell wall components, protein synthesis, and cell wall synthesis, respectively[8].

1.2.2 Active and latent infection. Besides poor patient compliance, *Mtb's* cell physiology during infection is another cause for difficulty in treating and clearing TB. *Mtb* can be found within a host in two possible infectious states: an active state in which the host shows symptoms and can proactively infect others, or a latent (dormant) state in which the host is asymptomatic and might never experience disease nor be able to spread *Mtb*. The data regarding the latent state is not included in many of today's statistics, which makes the actual infection rate of this bacterium even more alarming.

1.2.2.1 Active infectious state. *Mtb* infection first occurs by inhaling air droplets, which an individual with active TB disperses. These droplets containing the *Mtb* bacilli will then reach the new host's alveoli, where they can begin colonization. The host's innate immune response is often enough to kill this initial infection because immunocompetent individuals have a promising chance of fighting this infection[10]. If *Mtb* can survive this initial line of defense, it will continue replicating and cause a higher bacterial burden. In most cases, this sizeable bacterial burden will induce multicellular recruitment that will attempt to contain *Mtb* by forming a granuloma. However, depending on the severity of the infection, immature granulomas will only function as a temporary harbor for *Mtb* to persist and replicate. If the containment of *Mtb* fails, the bacilli can infect other organs, enter the bloodstream, and eventually return to the respiratory tract to be released. At this point, the human host is considered to have active TB and can easily infect others[11]. Although the *Mtb*-specific immune response is very complex and beyond my research scope, it is important to highlight *Mtb's* ability to evade the immune system so that it can cause disease or enter an indefinite dormant state.

1.2.2.2 Granulomas and Latent infectious state. Granulomas are the histological sign of an *Mtb* infection, commonly present during TB. At its most basic definition, granulomas are a dense accumulation of differentiated and blood-derived cells that enclose foreign bacteria to stop pathogenesis[12,13]. Inside the granuloma, *Mtb* will experience a variety of stressors, such as hypoxia, oxidative stress, and starvation[14]. For the longest time, granulomas were seen as host-protective structures for slowing down and blocking infections[15,16], which is the case for many asymptomatic TB patients who show evidence of granulomas in their X-rays[17]. Nevertheless, the fact that many individuals still experience and succumb to active TB shows that granulomas are

not always effective. As *Mtb* research continued, scientists discovered that granulomas can experience different transformations as the nodule matures. One example is the presence of necrotic areas known as *caseum*. Evidence shows that caseum is due to *Mtb*, which breaks down the granuloma and enables the bacteria to escape and enter a newly active state of infection. If the right opportunity arises, *Mtb* will gain access to the host's airway and likely continue to infect more individuals. Fortunately, depending on the individual's immune system, new white cells, like macrophages, can create a new granuloma to sequester *Mtb* again. If the host can control *Mtb* within the granuloma, the nodule calcifies and has a better chance of containing the bacteria[14,17]. This successful containment will force *Mtb* to enter a latent state of infection, which, depending on the host, can provide years to decades of protection.

1.2.3 Recap of Mtb and our research interest. *Mtb* causes the respiratory disease known as Tuberculosis during an active state of infection. Infected immunocompetent individuals can successfully clear Tuberculosis with the correct treatment plan and proper patient compliance. Those that fail to do so could enhance the opportunity for *Mtb* to become multi-drug resistant. Both active and latent states of infection provide *Mtb* with two different environments. *Mtb's* means of survival is characterized by its ability to "hide" from or inhibit processes involved in host immunity while simultaneously regulating cell growth in the presence of stressors and antibiotics. Because of this, there is still growing interest in the mechanisms that allow *Mtb* to adapt to stressful environments. In the Boutte lab, we are interested in understanding mycobacterial cell wall regulation in the presence of stress.

1.3 *Mycobacterium abscessus*.

1.3.1 Background. *Mycobacterium abscessus* (*Mab*) is an opportunistic, fast-growing, non-tuberculous mycobacterial pathogen that can be found in the environment. *Mab* is notorious for causing skin infections and infecting immunocompromised individuals with underlying lung diseases, such as individuals with cystic fibrosis[18]. More recently, however, it has been debated that due to its many virulence factors and its ability to survive on different human-made surfaces, *Mab* fits the standard of a true pathogen[19,20].

As with *Mtb, Mab* is difficult to treat due to its intrinsic ability to become drug-resistant to standard antibiotics. *Mab* has experienced many mutations through its survival in the environment, allowing it to develop the proper tools to defend itself against antibiotics. One example is the erm41 gene, which gives it resistance towards Clarithromycin, a widely used antibiotic to combat *Mab* soft-tissue infections[21].

1.3.2 Overview of Treatment. Because *Mab* can infect different types of organs, there needs to be more agreement and consistency regarding all aspects of treatment[22]. For example, *Mab* often survives as biofilms inside the lungs, which protects from environmental stressors like the host immune system and antibiotics. Pulmonologists usually disrupt the biofilm and then treat it with a combination of antibiotics, such as Amikacin and Cefoxitin, for about a year[22]. In the case of soft-tissue infection, like an ocular infection, topical treatment is the initial approach by using the antibiotics Amikacin and Clarithromycin, followed by surgical intervention if the disease is severe enough[5]. For more severe infections, physicians will suggest several weeks of combination therapy that generally includes a macrolide to affect bacterial protein synthesis

(Clarithromycin or Azithromycin), as well as intravenous medication, usually a combination of Amikacin and Cefoxitin/Imipenem, which affect protein and cell wall synthesis respectively.

1.3.3 Chapter 2 Rationale - The Stringent Response. For bacteria to survive changing environmental conditions, they must be able to adjust their cell physiology. The stringent response is a conserved stress mechanism in bacteria that allows many species to survive during stress by balancing many cellular processes, such as gene expression[23]. For most bacteria, this means reducing or suppressing the expression of growth-related genes and promoting the expression of stress-related genes. Through this type of regulatory mechanism, pathogenic bacteria like *Mtb* and *Mab* can survive in various stressful environments[24,25].

The molecular hallmark of the stringent response is the production of guanosine penta- and tetra-phosphate ((p)ppGpp)[26]. These stress signaling molecules, or alarmones, are responsible for the aforementioned "gene balancing" during stress conditions[27]. In *Escherichia coli (E.coli)*, the enzyme Rel is the synthase that catalyzes the production of (p)ppGpp. Meanwhile, an enzyme known as SpoT is known as the hydrolase that breaks down (p)ppGpp[28]. In other bacteria, Rel/SpoT homolog (RSH) proteins contain both synthase and hydrolase activity, such as in the case of Rel in *Mtb* (Rel_{Mtb}). Different clades of bacteria use (p)ppGpp differently across many stress conditions, such as in growth, starvation, or in the presence of antibiotics. This phenomenon partly concerns how (p)ppGpp interacts with different targets during stress. In some bacteria, like in *E.coli*, (p)ppGpp binds to RNA polymerase to promote or suppress the transcription of genes. While in others, its role could be more direct by binding to a wide variety of proteins to promote or inhibit their activity[29].

Based on current data, it can be suggested that the stringent response will contribute to cell survival in different ways, depending on the bacterial niche. This is specifically true in pathogenic bacteria, where the stringent response has been seen to contribute to cellular adhesion, invasion, biofilm formation, and immune evasion[27]. It is also essential to highlight the role of the stringent response regarding antibiotic tolerance and resistance. Since most drug treatments target cellular processes, like DNA replication and growth, it makes sense that downregulation of these targets would lead to diminished drug efficacy[30]. Therefore, understanding the mechanisms contributing to the stringent response is important when developing new drugs or therapies to treat infection and disease.

1.3.4 The Stringent Response in Mycobacteria. Mycobacteria like *Mtb* and *Mab* already possess an arsenal of genes that help them grow and survive specific stressors and antibiotics[31–35]. However, whether the stringent response regulates all or some of these genes has yet to be studied in these bacteria.

1.3.4.1 Stringent response in Mtb. To study the stringent response in *Mtb*, scientists mutated the rel gene so that the Rel protein would no longer be synthesized. This new strain was then called ▲rel$_{Mtb}$, which is a mutant that showed variability in survival across several stress conditions[24,25]. These studies focused on clinically relevant stressors such as active infection, oxygen deprivation, acidity, nutrient deprivation, oxidative stress, and antibiotic treatment. Results first showed that *Mtb* does follow a classical stringent response that accumulates (p)ppGpp in the presence of stress. These results showed that during exponential growth in

nutrient-rich media, basal levels of (p)ppGpp are detected[24], which suggests that even during a low-stress environment, the stringent response in *Mtb* contributes to cell survival.

1.3.4.2 Experimental approach in Mtb. Experiments regarding multiple stress conditions were performed between *Mtb* and ▲rel$_{Mtb}$. When tested in the presence of oxidative stress, acid stress, and antibiotics, these tests showed no difference between the two strains during a microdilution experiment. Although the antibiotic result was striking, future work showed opposite results[25], which suggests that microdilutions might not be a reliable way to test this stressor.
The ▲*rel*$_{Mtb}$ did show attenuated growth in typical lab growth conditions (complete nutrients; 37C) and at higher growth temperatures (42C), which suggests that the stringent response in *Mtb* contributes to thermoregulation and active growth. Other results showed that hypoxia and starvation were highly detrimental to ▲*rel*$_{Mtb}$ survival, which could explain how *Mtb* survives well within lung granulomas. These studies show that even within a specific environment, in this case, a mammalian host, the stringent response in *Mtb* is focused on defending the cell against particular stressors.

1.3.4.3 Stringent response in Mab. For *Mab*, no previous work has been done regarding *Mab*'s Rel protein and the stringent response. Similarly, as in *Mtb, Mab* has only one annotated RSH enzyme, and until proven differently, any current and future data is based on this one RSH. In contrast, there is data on the RSH and stringent response in the non-pathogenic *Mycobacterium smegmatis (M.smeg)*, but the presence of a small alarmone synthetase (SAS)[36] makes this model different from its pathogenic relatives. This SAS is called RelZ and is the second alarmone synthetase in *M. smeg's* stringent response. In addition to

specifically making ppGpp, RelZ also synthesizes pGpp, which has been seen to contribute to antibiotic tolerance in *M.smeg*. Our work shows that in our ▲rel$_{Mab}$ mutant, the cell can still produce (p)ppGpp, suggesting the presence of another alarmone synthetase. However, whether *Mab* has any other (p)ppGpp synthases has yet to be studied. We also found that the primary role of Rel$_{Mab}$ is to regulate growth metabolism, and not stress response genes.

1.3.5 Chapter 3 Rationale - Biofilms in Mab. *Mab* is commonly found living in aggregate communities known as biofilms. These communities are surrounded by an extracellular matrix that provides protection from environmental insults[37]. Inside biofilms, *Mab* can undergo physiological, metabolic, and, at times, genetic changes, which allow *Mab* to survive in different types of environments[37]. Hence, we can see biofilms as a stress response that aids *Mab* in colonizing, tolerating antibiotics, and evading the host's immune response[38–40].

1.3.5.1 Smooth and Rough morphologies. *Mab* can also be found in two different morphologies: a rough morphology, believed to be more invasive and virulent, and a smooth morphology, believed to be less invasive and mostly biofilm-forming morphology[41]. Studies have shown that this difference is due to the loss of glycopeptidolipids on the rough type, which could be a virulence strategy that leads to active disease[41]. Research reveals that the molecular basis for this switch is due to single nucleotide polymorphisms found in the *gpl* locus of the rough variant; a single nucleotide deletion in the *mmpL4b* gene, as well as a nucleotide insertion in the *mps1* gene[42,43]. Studies also showed that the rough morphology can persist and cause severe long-term infection, which can be partially attributed to an upregulation of genes known to cause persistence, specifically in the pathogenic relative *Mtb*[43]. Despite these attributes, something that

both variants have in common is that both can form biofilms. This conserved trait can be seen as an environmental strategy that can help *Mab* tolerate environmental stressors, such as antibiotics[44].

1.3.5.2 Correlation between Biofilm formation and nutrient availability. Research has shown that nutrient limitation does not only affect bacterial cell physiology but also the structure and mass of biofilms[45]. This is of specific importance regarding how pathogens use biofilms to survive in different environments. *Mab*, in particular, has been seen to colonize a wide range of extreme environments[46] (Galassi 2003 & Ghosh 2017—cant download from home). Our work focused on exploring and expanding on this idea, by comparing the physiology of biofilms grown in nutrients that mimic infection to biofilms grown in typical lab media. We reasoned that it is clinically relevant to understand how the composition of biofilms can affect their survival against stressors, such as antibiotics. We expect biofilms in the presence of different nutrients to differ in composition and antibiotic tolerance.

1.4 Mycobacterial cell wall regulation

1.4.1 The mycobacterial cell wall. Mycobacteria are known for their unique armor-like cell envelope, which contains four main layers: the cell membrane, cell wall core, surface lipids, and lastly, the capsule[47]. For every layer, numerous enzymes and their regulators are coordinated to maintain and control proper growth. This is notably true for the cell wall core, which consists of peptidoglycan, arabinogalactan, and mycolic acid layers. By having multiple layers, the mycobacterial cell wall has a very low permeability, a vital factor that contributes towards antibiotic resistance and tolerance in pathogens like *Mtb and Mab*[48].

1.4.2 Identifying Mycobacteria through its cell wall. Another unique quality of the cell wall is how it is identified through laboratory testing. Based on their cell wall composition, bacteria are commonly classified as either gram-negative or gram-positive, which has to do with the gram staining technique that helps identify them through a microscope; gram-positive cells are purple, and gram-negative are pink/red[49]. Although the mycobacterial cell wall has gram-negative and gram-positive qualities, they are classified as acid-fast. This has to do with how they are identified through an acid-fast stain that reacts with the mycolic acid layer; mycobacteria will turn red, while other bacteria will turn green/blue[50].

1.4.3 The Peptidoglycan layer: When properly built, the peptidoglycan (PG) layer provides cell shape, rigidity, and resistance against external stressors, such as turgor pressure[51]. The typical structure of PG across bacteria consists of glycan polymer strands that are crosslinked through short peptide stems[52] (intro-27-cant access PDF from home). These strands consist of chains of alternating sugars: N-acetyl-glucosamine (GlcNAc) and N-acetyl-muramic acid (MurNAc). Although this layer is conserved across bacterial species, there is variability in the composition and order of the peptide stems, which can affect the structure of the layer. These slight differences can promote structure variability in thickness, elasticity, and porosity in different growth conditions[51].

1.4.4 Building the PG layer, precursor biosynthesis. In order to form the PG layer, the production and transport of its precursor components need to be tightly regulated. The first step of this process is the committed formation of uridine diphosphate-N-acetylglucosamine (UDP-

GlcNAc) in the cytoplasm by the enzyme GlmU. Next, through a series of reactions in the cytoplasm involving a pair of Mur enzymes (MurA & MurB), UPD-MurNAc is synthesized from UDP-GlcNAc. Upon accumulation of UDP-MurNAc and the enzymatic activity of the remaining Mur enzymes (C through F), a pentapeptide stem is added to UPD-MurNac; this new compound is known as Park's nucleotide[53]. From this point, Park's nucleotide becomes membrane-bound by its translocation unto decaprenyl phosphate (C50-P) by the enzymatic activity of MurX (MraY), which now forms Lipid I[53]. Lastly, the final cytoplasmic step of PG precursor biosynthesis involve the formation of Lipid II by the glycosyltransferase MurG.

1.4.5 Lipid II translocation and polymerization. Once Lipid II is formed, it needs to be transferred from the cytoplasmic side of the inner membrane to the periplasm to be added to the growing PG layer. For this to occur, Lipid II interacts with the flippase MurJ, whose job is to flip Lipid II across the cytoplasmic membrane[54]. Once in the periplasm, Lipid II is then polymerized through transglycosylation of its disaccharides, followed by transpeptidation of its peptide stems. More specifically, transglycosylation is performed by glycosyltransferases (GTases) and transpeptidation by transpeptidases (TPases). Throughout bacteria, Penicillin-binding proteins (PBPs) are categorized as class A or class B, one group being able to perform both GTase and TPase reactions, while the other are only monofunctional with TPase activity, respectively. One type of monofunctional TPases are known as SEDS (shape, elongation, division, and sporulation) proteins. Both PBPs and SEDS proteins are part of large complexes that involve multiple enzymes and their regulators[47], which are needed to control proper PG layer assembly.

1.4.6 Regulation of PG synthesis. For *Mtb*, proper cell wall regulation is crucial for survival during infection[47]. It is important for cells to establish a strict coordination between growth and division that will not compromise cell integrity. This type of regulation requires multiple enzymes and regulators to work closely together to manage the production and assembly of the cell wall. Although all the cell wall layers in mycobacteria contribute to its resiliency as an organism, the PG layer is essential due to its role in cell shape and protection. Because of this, many studies have focused on the regulation and synthesis of the PG layer, and because it is an important target for antibiotics. One example of an essential component of PG synthesis is the cell wall regulator known as CwlM and its regulation of the PG precursor enzyme MurA.

1.4.7 Early literature on CwlM and its role as a PG hydrolase. In 2004, a group of researchers discovered a novel PG hydrolase in mycobacteria[55]. Due to its genetic homology to CwlB, a hydrolase in *Bacillus subtilis*, they named this protein CwlM. That study aimed to look into lytic enzymes (autolysins) that contributed to PG assembly, a subject not previously studied in *Mtb*. In that work, purified CwlM was used in specific assays to test and validate its role as a hydrolase of PG. In 2018, another group performed similar studies focusing on CwlM's hydrolytic contribution to autolysis and biofilm degradation in *Mtb* and *M.smeg*[56]. Despite both studies showing CwlM enzymatic activity, hydrolytic activity was not truly validated since proper experimental controls were not done in either study[56,57]. Other studies question CwlM's true enzymatic role due primarily to its cytoplasmic localization[58]. Meaning, how can CwlM act on PG if its not located in the periplasm, where the PG layer is located? Altogether, these early studies show that more work still needs to be done to validate CwlM's role as a PG hydrolase.

1.4.8 CwlM as a PG synthesis regulator. Using *M.smeg* as a model for *Mtb*, a more thorough investigation of CwlM through genetic and biochemical work showed its essential role as an activator of MurA, the first enzyme involved in PG precursor synthesis[58]. This study showed that CwlM is found in the cell's cytoplasm and that CwlM's activation of MurA occurs upon its phosphorylation by the essential Serine-Threonine Protein Kinase known as PknB. This work also highlighted how CwlM's activation of MurA differed in the presence or lack of nutrients. They showed that in starvation, CwlM is not phosphorylated, and does not activate MurA. In contrast, a similar experiment showed that the over-activation of MurA in starvation caused significant sensitivity towards clinically relevant antibiotics, highlighting the importance of this mode of regulation of cell wall synthesis in antibiotic tolerance.

Although it is not clear yet if CwlM has a role as a hydrolase, this study shows that CwlM's primary contribution is to regulate PG synthesis by activating MurA, an essential enzyme involved in PG synthesis.

1.4.9 Chapter 4 Rationale and Other Roles for CwlM. Previous cell wall research focused on reporting the critical role of the Serine-Threonine protein kinase PknB in mycobacteria (proposal 14). During this research, the authors identified CwlM as one of the primary substrates for PknB. Because CwlM has multiple threonine phosphorylation sites, studies were performed on the phosphorylated and non-phosphorylated forms of CwlM during active growth. They showed that depending on CwlM's phosphorylation state, CwlM appears to interact with at least two other proteins: the Lipid II flippase MurJ and the cell wall protein FhaA[59]. This calls attention to CwlM's significant and vital role in cell wall metabolism and make CwlM a promising drug target for future therapies against mycobacterial infections.

1.5 Summary and overarching research goal.

Mycobacteria encompasses many pathogenic species that cause detrimental diseases to humans. Mycobacteria's approach to dealing with environmental stressors, such as antibiotics, continues to make it an urgent bacterium to study, specifically how regulating its complex cell envelope contributes to survival and drug recalcitrance. Its co-evolution with humans has increased the likelihood of pathogens like *Mtb* to withstand medical intervention. Our lab believes that a better understanding of stress responses opens the door to developing better therapies and strategies to treat mycobacterial infections and diseases. The studies in this dissertation aim to highlight the importance of understanding mycobacteria's stress response, the importance of biofilms, and CwlM's essential contribution to the mycobacterial cell.

Chapter 2 - In *Mycobacterium abscessus*, the stringent factor Rel regulates metabolism, but is not the only (p)ppGpp synthase.

Augusto César Hunt-Serracín[1], Misha I. Kazi[1], Joseph M. Boll[1], Cara C. Boutte[1]

[1]Department of Biology, University of Texas, Arlington

2.1 Abstract

The stringent response is a broadly conserved stress response system that exhibits functional variability across bacterial clades. Here, I characterize the role of the stringent factor Rel in the non-tuberculous mycobacterial pathogen, *Mycobacterium abscessus* (*Mab*). I found that deletion of *rel* does not ablate (p)ppGpp synthesis, and that *rel* does not provide a survival advantage in several stress conditions, or in antibiotic treatment. Transcriptional data show that Rel_{Mab} is involved in regulating expression of anabolism and growth genes in stationary phase. However, it does not activate transcription of stress response or antibiotic resistance genes, and represses transcription of many antibiotic resistance genes. This work shows that there is an unannotated (p)ppGpp synthetase in *Mab*.

2.2 Importance

In this study, I examined the functional roles of the stringent factor Rel in *Mycobacterium abscessus (Mab)*. In most species, stringent factors synthesize the alarmone (p)ppGpp, which globally alters transcription to promote growth arrest and survival under stress and in antibiotic treatment. Our work shows that in *Mab,* an emerging pathogen which is resistant to many antibiotics, the stringent factor Rel is not solely responsible for synthesizing (p)ppGpp. I find that Rel_{Mab} downregulates many metabolic genes under stress, but does not upregulate stress response genes and does not promote antibiotic tolerance. This study implies that there is another critical but unannotated (p)ppGpp synthetase in *Mab,* and suggests that Rel_{Mab} inhibitors are unlikely to sensitize *Mab* infections to antibiotic treatment.

2.3 Introduction

Bacteria must adjust their physiology to permit survival in fluctuating conditions. The stringent response is a conserved signaling system that promotes survival of many species in stress and antibiotics by altering the transcription of about a quarter of the genome [60–64]. In this work, I profile the role of Rel, the sole annotated stringent factor, in the non-tuberculous, rapidly-growing *Mycobacterium abscessus* (*Mab*). *Mab* is an opportunistic pathogen that both lives in the environment, and causes skin and respiratory infections which are increasingly prevalent in Cystic Fibrosis patients [65]. *Mab* infections are difficult to treat due to intrinsic resistance to many antibiotics [22], and high tolerance under stress to almost all antibiotics tested [44,66]. One proposed strategy to help treat such antibiotic-recalcitrant infections is to inhibit regulatory systems, like the stringent response, which promotes antibiotic tolerance [30,67–69].

The conserved aspect of the stringent response is the synthesis, upon stress, of the hyperphosphorylated guanine (p)ppGpp. Once made, (p)ppGpp affects transcription in different ways [70–73] and also directly modulates replication [74,75], nucleotide metabolism [76–78], ribosome maturation [79,80] and translation [81–83].

There are a handful of different protein families that synthesize (p)ppGpp across bacterial clades. The most widely conserved are the Rel/Spo Homolog or RSH proteins, which contain, from N-terminus to C-terminus, a (p)ppGpp hydrolase domain, a (p)ppGpp synthase domain, and regulatory TGS and ACT domains [84]. Some RSH proteins associate with the ribosome and sense amino acid starvation by detecting when ribosomes have stalled due to an uncharged tRNA being in the A site [85,86]. Some RSH proteins detect other types of stress or nutrient deprivation via other mechanisms [87–90]. Many species have only one RSH-type protein, which is competent for both (p)ppGpp hydrolysis and synthesis [84]. Many species encode Small Alarmose Synthetase (SAS) and Small Alarmone Hydrolase (SAH) proteins, which contain only (p)ppGpp synthetase and hydrolase domains respectively [86,91–94]. Because SAS proteins do not have regulatory domains, they are typically controlled transcriptionally [86]. There are a few other (p)ppGpp synthesizing domains that have been preliminarily studied. ToxSAS proteins are part of toxin-antitoxin systems and synthesize (p)ppGpp as a toxin - these are found in both phage and bacterial genomes [95]. *Streptomyces antibioticus* has a polynucleotide phosphorylase (PNPase) which can also synthesize (p)ppGpp [96–99].

The physiological outputs of the stringent response vary across species, but there are conserved themes. First, the stringent response generally downregulates genes required for growth, such as ribosome and cell wall synthesis factors, and it alters transcription of central metabolism to prioritize survival rather than construction of new cells [61,62,73,100]. Stringent inhibition of growth

[24,26,100–104] indirectly protects against some stresses and antibiotics that interfere with growth factors. In many species, the stringent response upregulates stress response genes such as heat shock proteins, hibernation factors, and stress-specific transcription factors [62,105,106] and promotes survival in stress [69]. The stringent response also helps many bacteria survive through antibiotic treatment by promoting antibiotic tolerance [30].

The stringent response has been studied in *Mycobacterium tuberculosis* (*Mtb*) and *Mycobacterium smegmatis* (*Msmeg*). *Mtb* has one major (p)ppGpp synthetase, Rel$_{Mtb}$ which makes (p)ppGpp when respiration is inhibited, in stationary phase, and in total carbon and nitrogen starvation [24,107]. Rel$_{Mtb}$ also promotes survival of *Mtb* during nutrient and oxygen starvation, stationary phase [24] and chronic infection of mice [60] and guinea pigs [108,109]. Importantly, Rel$_{Mtb}$ also makes *Mtb* more tolerant to the first-line clinical antibiotic isoniazid during starvation and infection in mice [68]. A PNPase enzyme in *Mtb*, Rv2783, has been shown to have weak (p)ppGpp synthetase activity [110], and the *Mtb* genome contains another gene with a predicted GTP pyrophosphokinase domain, Rv1366. However, the Δ*rel*$_{Mtb}$ strain does not synthesize measurable (p)ppGpp in starvation conditions [24], so these other potential synthetases are either inactive or not activated in the conditions tested.

Msmeg has an RSH protein, Rel$_{Msmeg}$, which can both synthesize and hydrolyze (p)ppGpp [111–114]. Although the Δ*rel*$_{Msmeg}$ strain showed defects in biofilm formation and stationary phase viability, it can still synthesize (p)ppGpp [111,115]. The secondary (p)ppGpp synthetase, RelZ$_{Msmeg}$, has an RNaseHII domain in addition to the conserved SAS ppGpp synthetase domain [113], and also synthesizes pGpp [36]. Strains missing both synthetases have further biofilm and aggregation defects, but can still synthesize some (p)ppGpp [36], indicating that there is a third, uncharacterized synthetase in *Msmeg*.

In this study I examined the Δ*rel* strain of *Mab.* Rel$_{Mab}$ is an RSH protein. There are no other RSH genes, and no SAS genes in the *Mab* genome. I found that the Δ*rel*$_{Mab}$ strain still makes (p)ppGpp. The Δ*rel*$_{Mab}$ strain does not exhibit survival defects in several stress conditions including antibiotic treatment, but has a growth defect relative to wild type. I measured transcriptional changes in Δ*rel*$_{Mab}$ relative to wild type and found it helps downregulate many metabolic pathways in stationary phase.

2.4 Results

To explore the role of *rel*$_{Mab,}$ I built a strain of *Mab* ATCC19977 with a deletion of the *rel* gene (MAB_2876), which has the canonical RSH gene structure, including a (p)ppGpp hydrolase domain, a (p)ppGpp synthetase domain, a TGS domain and an ACT domain. I measured (p)ppGpp in both the wild-type *Mab* and Δ*rel*$_{Mab}$ strains, in logarithmic phase and carbon starvation (Fig. 2.1). I found that both the wild-type and Δ*rel*$_{Mab}$ strain produce (p)ppGpp in both log. phase and starvation, and the amount of ppGpp is increased in both strains in starvation.

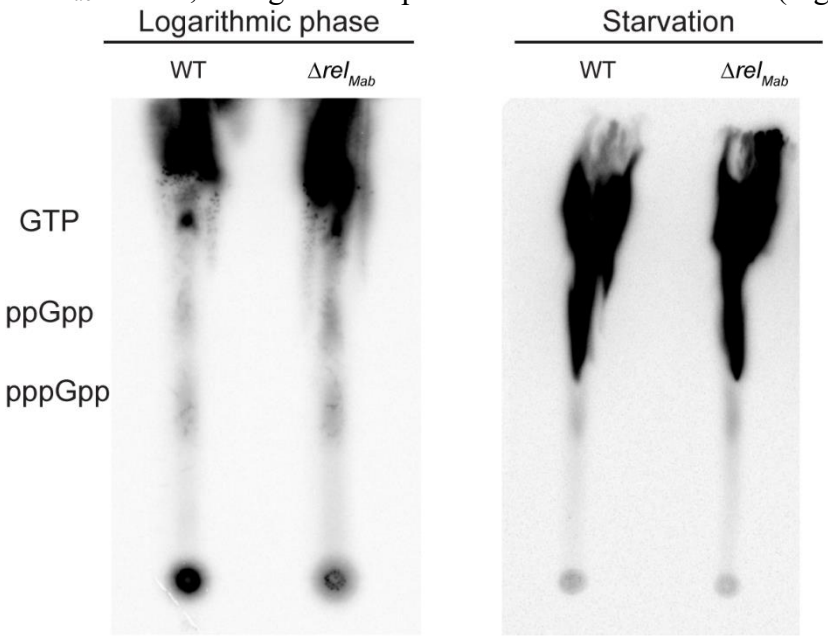

Figure. 2.1. Thin-layer chromatography (TLC) of nucleotides extracted from M. abscessus strains. Guanine nucleotides extracted from ^{32}P-labeled *M. abscessus* strains from logarithmic phase and starvation.

In many species, *rel* orthologues promote survival during stress conditions, such as stationary phase, acid stress, starvation, or oxidative stress [24,64,91,103,116,117]. To evaluate the physiological role of *rel* in *Mab*, I assayed survival of wild-type, Δ*rel*$_{Mab}$ and complemented strains upon and after transfer to either carbon starvation (Fig. 2.2A), salt stress (Fig. 2.2B), oxidative stress, (Fig. 2.2C) or acidic media (Fig. 2.2D). Treatment with these stressors did not induce measurable differences in growth or survival of Δ*rel*$_{Mab}$ relative to wild-type and the complemented strain. Thus, Rel$_{Mab}$ does not regulate responses to these stresses under the conditions tested, or at least not enough to affect growth or survival.

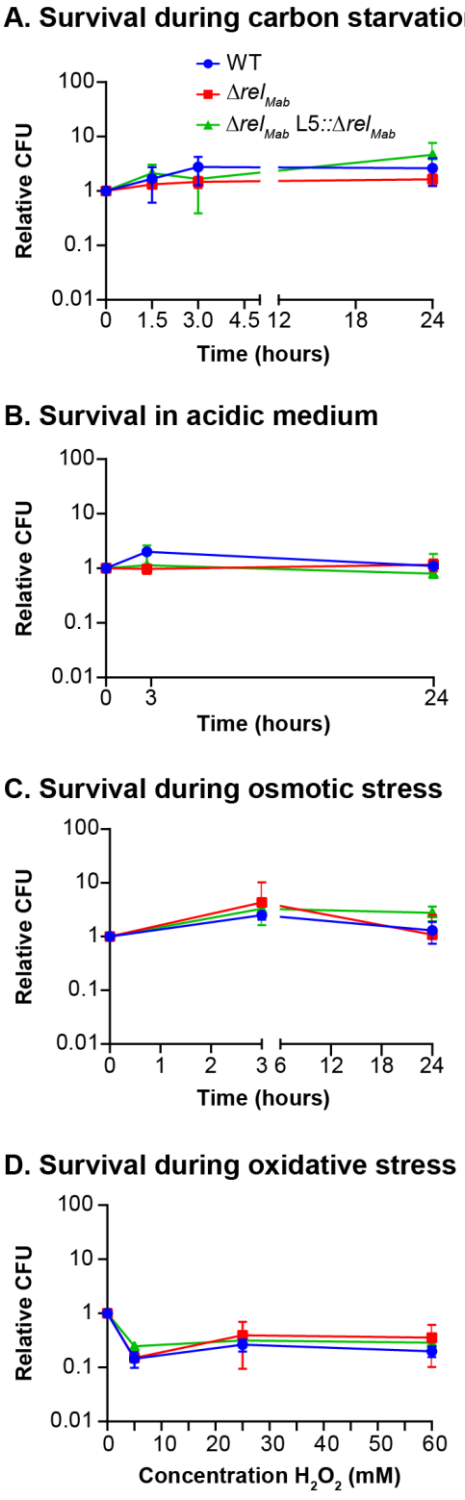

Figure 2.2. Contribution of *rel*$_{Mab}$ to survival in various stresses. (A) Colony-forming units (CFU) of wild type *Mycobacterium abscessus* strain ATCC19977 (blue), Δ*rel*$_{Mab}$ (red), and the complemented strain Δ*rel*$_{Mab}$ L5::*rel*$_{Mab}$ (green) in Hartman's du Bont medium with no glycerol and Tyloxapol as a detergent. (B) CFU in 7H9 Middlebrook medium with a pH of 4. (C) CFU in Lennox LB with 1M of NaCl. (D) CFU in Hartmans du Bont medium with 5mM, 25mM or 60mM of tert-butyl peroxide after 24 hours. Relative CFU is calculated by taking the ratio between each CFU value and the initial CFU value at time zero. All data points are an average of three biological replicates. Error bars represent standard deviation. There are no significant differences in any of these data by a two-tailed student's t-test.

I also found that Rel*Mab* does not promote survival in stationary phase (Fig. 3A). Robust survival in the Δ*relMab* in all stress conditions is likely aided by the continued synthesis of (p)ppGpp under stress (Fig. 2.1). Growth curves showed that Δ*relMab* had a significant growth defect relative to wild type and complemented strains (Fig. 2.3B).

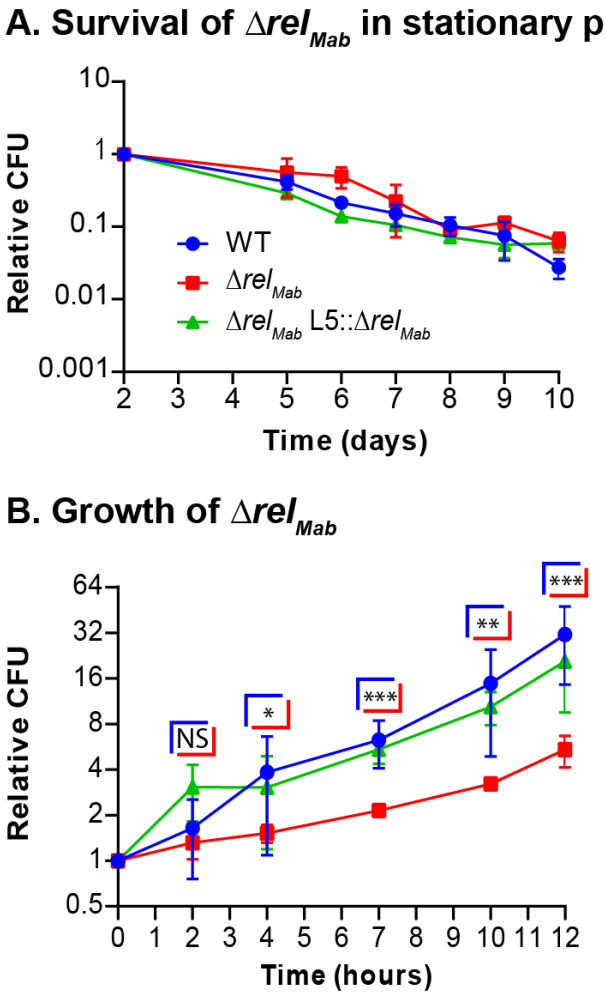

Figure 2.3. Growth and stationary phase survival of Δ*relMab* . (A) Colony-forming units (CFU) in stationary phase in 7H9 media. The 2-day time point is 48 hours after diluting logarithmic phase cultures to OD_{600}=0.05. (B) CFU during logarithmic phase growth in 7H9 medium. Graph is set at a log2 scale. Doubling-times ± 95% confidence interval = wild type 2.15 h ± 0.08; Δ*relMab* 4.67 h ± 4.26; Δ*relMab* L5::*relMab*; Δ*relMab* L5::*relMab* 2.84 ± 1.85. *P*-values are for the wild-type compared to Δ*relMab*. *P*-values for *t*=4, *P* = 0.0415; *t*=7, *P* = 0.00015; *t*=10, *P* =0.006; *t*=12, *P* =0.00029. *P*-values between wild-type and the complemented strain were not significant. *P*- values between strains in stationary phase were not significant (data not shown). Asterisks represent significance as measured by the two-tailed student's *t* -test; * = $P \leq 0.05$; ** = $P \leq 0.01$; *** = $P \leq 0.001$; n.s. = $P > 0.05$.

Because the stringent response is a major activator of antibiotic tolerance and persistence in many species [64,118,119], I sought to assess how Rel contributes to antibiotic tolerance in *Mab.* First, I treated *Mab* cultures in logarithmic phase with amikacin, clarithromycin and cefoxitin, which are commonly prescribed to treat *Mab* infections [120]. I found that clarithromycin and cefoxitin alone were ineffective against all of the strains (Fig. 4A). However, amikacin treatment resulted in 10-100-fold decrease in viability of wild-type and complemented strains, but had no effect on Δ*rel*$_{Mab}$.

Antibiotic tolerance increases in stationary phase in most bacterial species relative to logarithmic phase [64,121]. I repeated the antibiotic survival experiments on cultures in stasis and found that Rel$_{Mab}$ does not affect tolerance to clarithromycin or cefoxitin (Fig. 2.4B). Similar to amikacin treatment in growth, Rel$_{Mab}$ increased susceptibility relative to wild type and the complemented strains in stasis.

A major function of the stringent response in other bacteria is to regulate transcription [63]. To determine the effects of Rel$_{Mab}$ on transcription, I compared the trancriptome of wild-type and Δ*rel*$_{Mab}$ in both logarithmic and stationary phases using RNASeq. I found that Rel$_{Mab}$ represses many more genes than it activates.

In logarithmic phase (OD=0.5), when Δ*rel*$_{Mab}$ grows more slowly relative to wild type (Fig. 2.3B), I found 150 genes repressed by *rel*$_{Mab}$ in the wild-type strain at least 3-fold, and only 7 genes were activated. The only annotated upregulated genes are an efflux pump (MAB_0677) and a major facilitator superfamily (MFS) transporter (MAB_0069). I found several *mce* family genes that were repressed by *rel*$_{Mab}$. Mce proteins are typically lipid transporters, but they also play roles in host cell entry and immune modulation [122]. I also found two antibiotic resistance genes that are repressed by *rel*$_{Mab}$ in logarithmic phase (Table 2.1).

Even though there was no apparent difference in survival between the wild-type and Δ*rel*$_{Mab}$ strains in stationary phase, I observed significant differences in transcription. I isolated RNA from stationary phase cultures that were shaken for 48 hours after being diluted to OD=0.05. I found hundreds of genes that were repressed by *rel*$_{Mab}$ in the wild type strain in stationary phase, but none that were activated by *rel*$_{Mab}$ 3-fold or more. I found many genes in the WhiB7 regulon (Table 2.1) which are repressed in stationary phase, though they are mostly unaffected in logarithmic phase. WhiB7 is a transcription factor that activates many antibiotic resistance genes and promotes resistance to many classes of antibiotics in *Mab* [35]. It is notable that these antibiotic resistance genes are repressed by *rel*$_{Mab}$ in stasis, which would imply that wild type *Mab* would be more susceptible to antibiotics in this condition, which is what I see in amikacin treatment. In the case of clarithromycin and cefoxitin, increased tolerance through downregulation of target expression may counterbalance the repression of the antibiotic resistance genes, resulting in no differences in susceptibility in our assays (Fig. 2.4).

Table 2.1. Antibiotic Resistance Genes – (Under whiB7 regulon)*

***Mab* GENE Annotation**	**FC-Δ*rel*$_{Mab}$/ vs. WT LOG**	**FDR-corrected *P* value Δ*rel*$_{Mab}$ / vs. WT LOG**	**FC-Δ*rel*$_{Mab}$ / vs.WT Stat.**	**FDR-corrected *P* value Δ*rel*$_{Mab}$ / vs. WT Stat.**	**FC-WT.stat/ WT.log**	**FDR-corrected *P* value WT.Log vs. WT.Stat**	**Mab GO. Mol. function**
MAB_0163c	+2	1.1E-04	+40	5.1E-12	+2	1.7E-311	Aminoglycoside Phosphotransferase

MAB_0185c	+1	0.3	+5.4	6.4E-03	-5.4	0	Arabinosyl Transferase*
MAB_0186c	+1	0.8	+9.7	1.8E-04	-7.4	0	Arabinosyl Transferase*
MAB_1341	+1	0.45	+34	2.3E-11	-1.3	5.5E-13	Decarboxylase*
MAB_1342	+1.4	0.03	+14	0	-1	0	Acyl-CoA synthetase*
MAB_1395	+2.7	1.3E-04	+48	5.2E-10	+1	7.2E-29	Transporter*
MAB_1396	+2.5	3.7E-06	+36	0	-1	0	Multidrug MFS transporter
MAB_1846	-1.3	0.44	+28	4.2E-06	-1.4	2.9E-265	ABC transporter*
MAB_2273	+2.3	8.8E-12	+101	1.96E-08	+2.2	0	MFS transporter*
MAB_2297	+1.5	0.02	+99.2	7.1E-08	-2.1	0	Methyltransferase-erm41*
MAB_2310	+1.3	0.5	+5.7	0.03	+3.6	1.5E-50	Multidrug transporter
MAB_2355c	+2.2	1.5E-08	+17	0	+2.8	0	ABC transporter*
MAB_2396	+2.1	8.2E-03	+18	7.3E-09	+1.5	4.5E-122	Probably acetyltransferase*

MAB_2640c	+1.2	0.122	+5	5.4E-03	-2.4	0	Mmr - multidrug transport integral membrane protein
MAB_2736c	+1	0.6	+13	1.99E-10	-3.7	0	ABC transporter
MAB_2780c	+1.7	0.01	+27	1.14E-07	+3.3	0	MFS transporter*
MAB_2807	-1	0.7	+5	4.4E-03	-4.7	0	MFS transporter
MAB_2875	+5.4	9.7E-06	+38	0	+1.2	1.6E-171	Beta-lactamase
MAB_2989	+2	5.1E-04	+6.8	2.9E-05	+2.93	1.1E-222	Chloramphenicol acetyltransferase
MAB_3042c	+2.7	1.9E-12	+24	0	+1.82	0	GTpase-Hflx*
MAB_3467c	+6	2.5E-03	+21	0	+92	0	Heat shock protein*
MAB_3508c	+1.8	0.3	+31	0.08	+14	0.38	WhiB7
MAB_3762	+2	2.4E-09	+11	2.9E-10	+7.09	4.9E-143	Membrane protein*
MAB_3869c	-1.3	0.158	+6.7	5.4E-03	-1.67	0	DNA directed RNA polymerase*
MAB_4294	+1.8	3.1E-03	+28	0	+1.88	0	Aminotransferase*
MAB_4395	+2.4	0	+8	8.8E-07	+1.1	0	Aminoglycoside-2’-N-acetyltransferase

MAB_4837	+4.6	0	+26	0	+1.84	1.9E-312	Aminoglycoside phosphotransferase

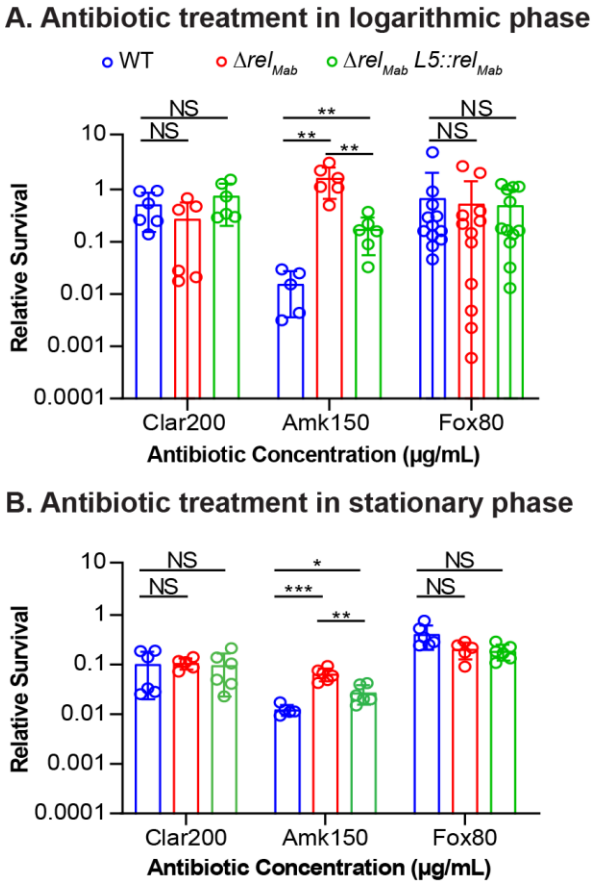

Figure. 2.4. Contribution of *rel*$_{Mab}$ to survival in antibiotic treatment. Relative Colony-forming units (CFUs) of strains treated with either 200 µg/mL of clarithromycin (Clar), 150 µg/mL of amikacin (Amk), or 80 µg/mL of cefoxitin (Fox) for either (A) 48 h in logarithmic phase or (B) 72 h in stationary phase. Relative CFUs were calculated by taking the ratio between the CFU value after treatment and the initial CFU value at time zero. The bars represent the mean of 6-9 biological replicates, the individual values are shown by the dots. Error bars represent standard deviation.

Logarithmic phase *P*-values: (Amk150) WT vs. Δ*rel*$_{Mab}$ = 0.005; WT vs. Δ*rel*$_{Mab}$ L5::*rel*$_{Mab}$ = 0.01; Δ*rel*$_{Mab}$ vs. Δ*rel*$_{Mab}$ L5::*rel*$_{Mab}$ = 0.004 . Stationary phase *P*-values: (AMK150) WT vs Δ*rel*$_{Mab}$ = 0.00017; WT vs. Δ*rel*$_{Mab}$ L5::*rel*$_{Mab}$ = 0.0217; Δ*rel*$_{Mab}$ vs. Δ*rel*$_{Mab}$ L5::*rel*$_{Mab}$ = 0.0017. Asterisks represent significance as measured by the two-tailed student's *t* -test; * = $P \leq 0.05$; ** = $P \leq 0.01$; *** = $P \leq 0.001$; n.s. = $P > 0.05$.

I also found several cell wall biosynthetic genes that are downregulated by *rel*$_{Mab}$ in stationary phase. Downregulation of growth factors is typical in stringent responses across many bacterial species [62,101,119,123,124]. I see that *rel*$_{Mab}$ downregulates many central metabolism genes in stationary phase (Fig. 2.5), which shows that when Rel is present, it contributes to the decrease in central carbon metabolism during stress. However, it is notable that not all the genes in a given pathway are downregulated equally. I hypothesize that this uneven regulation of certain pathways may allow certain metabolites to accumulate and be re-directed to other pathways. In a metabolic pathway where most of the enzymes are downregulated, I expect that the product of a single gene that is not downregulated will accumulate. I note that many of the metabolites I expect to accumulate converge on the NAD synthesis pathway. In addition, none of the genes in the NAD synthesis pathway are downregulated by *rel*$_{Mab}$, which implies that continued metabolism of NAD, which is a critical cofactor in many pathways, may be important in stationary phase.

From our preliminary analysis, Rel$_{Mab}$ helps regulate growth and central metabolism, and affects expression of antibiotic resistance genes; however, it does not seem to upregulate specific stress responses in the conditions tested.

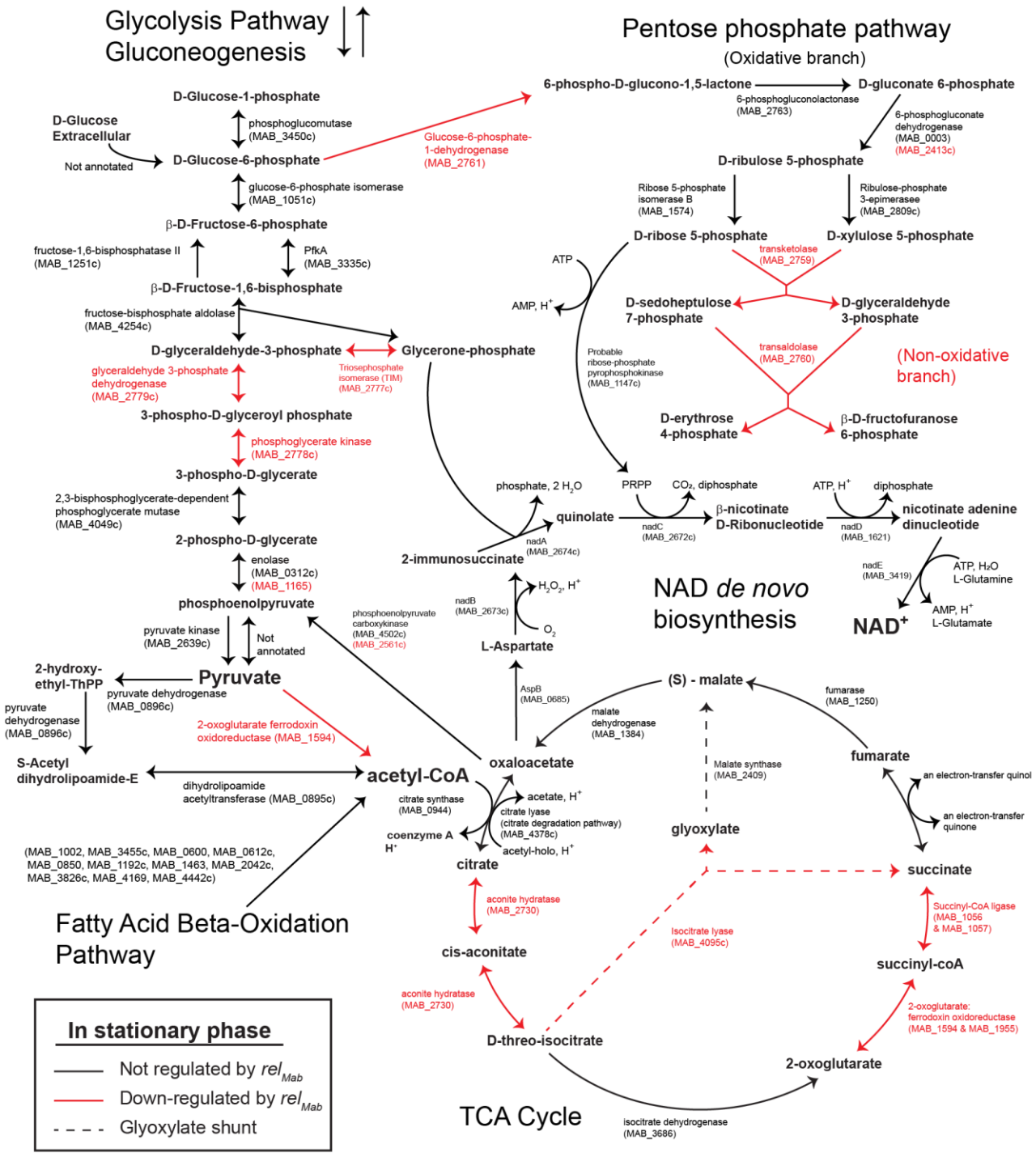

Figure 2.5. Repression of central metabolic genes by Rel$_{Mab}$ during stationary phase. Genes in red are downregulated by Rel$_{Mab}$ at least 3-fold in stationary phase, $P < 0.05$. Genes in black are not significantly regulated by Rel$_{Mab}$ in stationary phase. See Table S4 for data.

2.5 Discussion

Mtb, Msmeg and *Mab* all have a stringent response, but they have evolved use of different sets of genes to synthesize the same alarmone. The *Mab* genome encodes only one annotated RSH gene, rel_{Mab} (MAB_2876), and no homologs of SAS or SAH genes. rel_{Mab} is homologous to RSH genes in *Mtb* and *Msmeg*. I found that the Δrel_{Mab} strain could still produce (p)ppGpp, consistent with the presence of an unannotated (p)ppGpp synthase. *Mab* does not have a homolog of the SAS-RNaseHII *relZ*, which has been characterized in *Msmeg* [36,111,113]. Despite this, *Msmeg* and *Mab* are similar in having significant (p)ppGpp synthesis in the absence of the RSH gene (Fig. 2.1) [107], and in exhibiting greater survival with some antibiotics (Fig. 4) [115,121]. *Mab* does have a homolog of the PNPase which has been shown to be capable of (p)ppGpp synthesis in *Mtb* (MAB_3106c) [110]. MAB_3106c is transcriptionally upgregulated 4-fold in the Δ*rel* strain compared to wild-type in stationary phase, indicating that the presence of Rel may decrease the need for transcription of this gene. In the wild-type strain, this gene is also upregulated ~7 fold in stationary phase compared in log. phase, indicating that this gene is used in stress. I therefore propose MAB_3106c as a possible additional (p)ppGpp synthase.

Our results show that the stringent factor Rel_{Mab} does not promote survival during *in vitro* stress, though it does promote growth during logarithmic phase (Fig. 2.2, 2.3A). Our transcriptomics analysis corroborates these results, as they indicate that Rel_{Mab} does not upregulate stress response genes, but does alter transcription of growth metabolism genes. It is possible that increases in (p)ppGpp stimulate transcription of stress response genes in *Mab*, as is seen in other species [62,106,125,126] – our experiments did not test this because in our assays Δrel_{Mab} synthesizes comparable amounts of (p)ppGpp as wild-type (Fig. 2.1). The unannotated ppGpp synthase may contribute to stress response signaling. Our transcriptional data show that Rel_{Mab} is involved in

downregulating metabolism for growth arrest (Fig. 2.5) even though (p)ppGpp levels are still present in the Δ*rel*$_{Mab}$ strain. There is precedent for metabolic genes being regulated separately from stress response genes in the stringent response. In *E. coli*, some metabolic genes are repressed at a lower (p)ppGpp level than is required to induce a regulon of stress response genes[127]. (p)ppGpp likely does not directly bind RNAP in mycobacteria as it does in *E. coli* [128], and it is currently unknown how it exerts its effects on transcription. Further knowledge of the functioning of the mycobacterial stringent response will be required before I can speculate about the mechanism by which (p)ppGpp could differentially affect transcription of metabolic and stress response genes in *Mab.*

Mab is notorious for having resistance to many clinical antibiotics and expressing many antibiotic resistance genes [35,129,130], which is why it is problematic to treat infections in cystic fibrosis patients [131]. I observed in our transcriptional data that Rel$_{Mab}$ downregulated numerous antibiotic resistance genes in stationary phase (Table 2.1). In other species RSH proteins promote antibiotic tolerance [64,68,119] and sometimes also increase expression of antibiotic resistance genes [132,133]. Studies are ongoing to find drugs that would inhibit (p)ppGpp synthesis by RSH proteins [68,69], as such drugs are expected to increase susceptibility to clinically available antibiotics. Our results indicate that Rel$_{Mab}$ inhibitors, should they become available, are unlikely to help treat *Mab* infections. Instead, efforts should focus on identifying the other (p)ppGpp synthetase(s) in *Mab* so that it can be explored as a drug target.

2.6 Materials and Methods

2.6.1 Construction of strains. Primers 1233 – 1238 (Table S3) were used to amplify a 502 bp segment upstream of *Mab rel* which included the start codon, a 448 bp segment downstream of Mab *rel* which included the stop codon, and a 788 bp ZeoR cassette. All 3 segments were stitched together by PCR to form the Δ*rel*::zeoR double stranded recombineering knockout construct. Δ*rel*$_{Mab}$ was generated through double stranded recombineering, as previously described [134]. Colonies from the transformation of the Δ*rel*::zeoR construct were PCR checked by using primers 1424-761, 1235-1236, and 762-1425 (Fig. S1A). To make the complemented strain, the *rel*$_{Mab}$ gene was amplified through PCR using primers 1329-1330 and inserted into pKK216 [135] with NdeI and HindIII. This new plasmid, pCB1248, was transformed into the Δ*rel*$_{Mab}$ mutant strain in order to create the complementation strain, Δ*rel*$_{Mab}$ *L5::rel*$_{Mab}$, in which *rel*$_{Mab}$ expression is driven by a constitutive promoter (BN17, Fig.S1B).

2.6.2 Media and culture conditions. All *M. abscessus* ATCC 19977 wild-type and mutant cultures were started in 7H9 (Becton, Dickinson, Franklin Lakes, NJ) medium with 5 g/liter bovine serum albumin, 2 g/liter dextrose, 0.85 g/liter NaCl, 0.003 g/liter catalase, 0.2% glycerol, and 0.05% Tween 80 and shaken overnight at 37° C until cultures entered logarithmic phase. For starvation and other specific assays, Hartmans-de Bont (HdB) minimal medium was made as described previously [136]. Cultures were inoculated to OD_{600} 0.05, unless otherwise stated. All CFU time points were plated on Luria-Bertani (LB) agar and placed in 37° C incubator for 4 days.

2.6.3 Mab (p)ppGpp extraction and detection. *Mab* strains were grown until logarithmic phase (OD_{600} 0.5) in homemade 7H9 medium. To maximize ^{32}P-labeling, 7H9 medium with 1/25 of

normal phosphate levels was used [24]. Logarithmic phase *Mab* cells were pelleted and resuspended in 1mL of low phosphate 7H9, followed by the addition of ^{32}P-labeled orthophosphoric acid to a final concentration of 100 µCi/mL. ^{32}P-labeled cells were then incubated at 37° C and shaken at 200 rpm for 4 h. Following incubation, cells were pelleted and resuspended with 100 µL of TBST (Tris-buffer saline pH 8, with 0.05% Tyloxapol), and treated with 1 mg/mL of lysozyme on ice for 20 minutes. Equal volume 2 M Formic acid was then added to each sample, followed by a 5 minute centrifugation at max speed. Supernatant was then collected for each sample and stored in -20° C. For starvation cultures, a second set of log phase *Mab* strains (OD_{600} 0.5) were washed and resuspended in TBST. Addition of ^{32}P-labeled orthophosphoric acid, and (p)ppGpp extraction was performed similarly as logarithmic phase cultures.. Following extraction, 20 µL of extract from all cultures were spotted on PEI-cellulose TLC plates and developed in 1.5 M Potassium monophosphate buffer (pH 3.4). The plates were then air dried and placed on a phosphor screen (Molecular dynamics) overnight. The phosphor screens were scanned with a Storm 860 scanner (Amersham Biosciences) and images were analyzed with ImageQuant software (Molecular Dynamics).

2.6.4 Δrel_{Mab} *stress assays***.** For all stress assays, strains were prepared and grown into logarithmic phase. Unless otherwise stated, cultures for stress assays were done in 24-well plates and shaken at 130 rpm at 37° C. For carbon starvation, strains were inoculated in 30 mL inkwells in HdB minimal media with no glycerol, and with Tyloxapol as a detergent. For acid stress, strains were inoculated in 7H9 medium pH 4. For osmotic stress, strains were inoculated in LB broth medium with 1M salt (ACS Sodium Chloride, VWR Chemicals BDH). For oxidative stress, all strains were inoculated in complete HdB minimal medium, which does not contain catalase, and strains

were exposed to different concentrations of tert-Butyl Hydroperoxide (Alfa Aesar). CFU time points were taken upon inoculation, at 1, 3, and 24 h post-inoculation.

2.6.5 ΔrelMab growth curve and stationary phase survival. Log-phase cultures of all strains were inoculated to OD 0.05 in 30 mL inkwells in 7H9 media. Cultures were then placed in shaking incubator at 37° C and 130 rpm. CFU time points were then taken throughout a 12-hour period. For stationary phase survival, a second set of cultures were grown into stationary phase up to 48 h. Initial CFU time-point was taken at 48 h after dilution of logarithmic phase samples to OD_{600} 0.05, with subsequent time points taken at 5, 6, 7, 8, 9, and 10 d.

2.6.6 Antibiotic assays. For the logarithmic phase experiments, strains were kept in logarithmic phase in 7H9 for *t*~24 h and diluted to OD_{600} 0.05 and treated with either 150 µg/mL of amikacin, 200 µg/mL clarythromycin, or 80 µg/mL of cefoxitin. These antibiotic concentrations were chosen because they were shown in a previous study to cause killing of *Mab* in certain conditions [66]. CFUs were measured upon treatment (*t*=0) and 48 h after treatment (*t*=48). For stationary phase, logarithmic phase cells at OD_{600} 0.05 were shaken for 48 h and then treated as above. CFUs were measured upon treatment and 72 h after treatment.

2.6.7 RNA isolation, library preparation and data analysis. RNA from three biological replicates of each strain and condition was isolated as previously described [137] with some modifications. After growth for *t*~24 hours in either logrithmic or stationary phase, cells were transferred to 15 mL conical tubes and centrifuged at 4° C for 3 min at 1467 x g. Cell pellets were immediately resuspended in 750 µl of TriZol (Invitrogen) and lysed by bead beating. RNA was purified

according to protocol with the Zymogen Direct-zol RNA Miniprep Plus (cat. No 2070). RNA was processed for Illumina sequencing using the TRuSeq Total RNA Library Prep from Illumina, with bacterial rRNA removal probes provided separately by Illumina. Sequencing was performed using Illumina NovaSeq at the North Texas Genome Center at the University of Texas in Arlington.

Between 50-300 million pair-end reads per library were mapped to the *M. abscessus subs. abscessus* strain ATCC 19977 published genome using CLC Genomic Workbench software (Qiagen). To minimize the skewing effect that certain PCR jackpots had on the data, we adjusted the number of reads mapped from each library so the median reads per gene were equivalent within an experiment. In the logarithmic phase samples, the median reads per gene was ~600. In the stationary phase samples, the median reads per gene was ~100. After normalization, the Reads Per Kilobase Million (RPKM) values were determined for each gene, and the weighted proportion fold change of RPKM between wild type and Δrel_{Mab} for each condition were calculated by CLC Workbench. The Baggerley's test was used to generate a false discovery rate corrected P-value. We used an arbitrary cut-off of 3-fold change with a false-discovery rate corrected $P \leq 0.05$ to identify significantly differentially regulated genes between wild type and Δrel_{Mab} in each condition. Because the median reads per gene for logarithmic phase samples was 6 times higher than for stationary phase samples, we linearly scaled the fold-change values when comparing logarithmic to stationary phase data to normalize for this difference in read depth.

2.6.8 Real-time PCR (Supplemental data included in published work). For RNA-seq validation, real-time PCR (RT-PCR) was performed with the Kapa Biosystems Sybr Fast One-Step qRT-PCR kit. RNA was extracted in triplicates from each *Mab* strain as previously described. Primers for reverse-transcription (RT) were designed for each gene of interest by using Primer3 (Table S3).

Each 20 µL RT reaction mixture contained 10 µL One-step SYBR green Master Mix, 1 µL of each primer, 4.5 µL nuclease-free water, 0.5 µL of qScript One-step RT, and 3 µL of RNA. RT-PCR was done by using Bio-Rad CFX Connect Real-time system. The relative target levels (fold change) were calculated using the ΔΔCt method [138], with normalization of RNA targets to TetR transcription factor gene (MAB_1638).

Acknowledgements. This work was funded by a Pilot and Feasibility Award from the Cystic Fibrosis Foundation to CCB and by funding from the National Institutes of Health (grant AI1468269 and GM143053 to JMB).

Chapter 3 - Biofilm-associated *Mycobacterium abscessus* cells have altered antibiotic tolerance and surface glycolipids in Artificial Cystic Fibrosis Sputum Media.

Augusto Cesar Hunt-Serracin[1], Brian J. Parks[1], Joseph Boll[1] and Cara Boutte[1*]

[1]Department of Biology, University of Texas Arlington

[*]Corresponding author: cara.boutte@uta.edu

3.1 Abstract

Mycobacterium abscessus (*Mab*) is a biofilm-forming, multi-drug resistant, non-tuberculous mycobacterial (NTM) pathogen increasingly found in Cystic Fibrosis patients. Antibiotic treatment for these infections is often unsuccessful, partly due to *Mab*'s high intrinsic antibiotic resistance. It is not clear whether antibiotic tolerance caused by biofilm formation also contributes to poor treatment outcomes. I studied the surface glycolipids and antibiotic tolerance of *Mab* biofilms grown in Artificial Cystic Fibrosis Sputum (ACFS) media in order to determine how they are affected by nutrient conditions that mimic infection. I found that *Mab* displays more of the virulence lipid trehalose dimycolate when grown in ACFS compared to standard lab media. In ACFS media, biofilm-associated cells are more antibiotic tolerant than planktonic cells in the same well. This contrasts with standard lab medias, where biofilm and planktonic cells are both highly antibiotic tolerant. These results indicate that *Mab*

cell physiology in biofilms depends on environmental factors, and that nutrient conditions found within Cystic Fibrosis infections could contribute to both increased virulence and antibiotic tolerance.

3.2 Introduction

Infections caused by Non-Tuberculous Mycobacteria (NTM) are on the rise across the globe[139,140]. *Mycobacterium abscessus* (*Mab*) is a highly antibiotic-resistant NTM that causes soft tissue infections and is an increasingly common respiratory pathogen in Cystic Fibrosis (CF) patients[131,141]. While most NTM infections are believed to be contracted through environmental exposure, *Mab* has recently been shown to be transmitted between CF patients, probably by fomites[142]. Unfortunately, *Mab* infections in CF patients are very difficult to treat, and there are no standardized treatment regimens. Treatment usually involves some combination of clarithromycin, amikacin, imipenem, cefoxitin and/ or linezolid[143]. Infection clearance after up to 3 years of antibiotic treatment is achieved in only 10-55% of patients[143]. This level of treatment failure is likely partly due to intrinsic antibiotic resistance[33,35,144]; however, antibiotic tolerance may also play a role[145], though the environmental conditions that induce tolerance in this organism are poorly understood.

The pathophysiology of *Mab* infection in the CF lung has scarcely been studied, but one pathology study of explanted lungs from CF patients showed *Mab* aggregates that appear to be forming a biofilm around the alveoli[146]. Biofilms are bacterial communities that in many species are held together by exopolysaccharides[147]. Mycobacterial biofilms appear to depend on surface glycolipids[148] and free mycolic acids[149,150], though many questions remain about the composition of the matrix in mycobacterial biofilms. Because bacteria growing in biofilms are notoriously tolerant to antibiotics[151], this mode of growth during infection may contribute to the treatment

recalcitrance of *Mab*. While I currently lack a comprehensive model of the chemical and genetic basis of *Mab* biofilm formation, it is clear that surface glycolipids are important. Glycopeptidolipids, which are found on the outer leaflet of the mycobacterial outer membrane, have been shown to affect biofilm structure[44] and are thought to modulate the course of infection[42,152]. Trehalose dimycolate (TDM), which is known to contribute to virulence in *Mtb*[153] are also found on the surface of some *Mab* strains, though its contribution to biofilm formation and virulence in *Mab* has not been studied.

Mab has two genetic isoforms: the wild-type "smooth" strains, which produce abundant GPLs and minimal TDM, and "rough" mutants, which have genetic lesions in the GPL loci and display little or no GPLs but sometimes have higher levels of TDM[41,154]. The smooth strains form more robust biofilms and it is thought that this form could contribute to colonization at infection sites[41], which is likely promoted by GPLs masking other cell surface molecules that activate innate immunity[152]. The rough mutants cause more inflammation[152], are more virulent, and are thought to promote more tissue invasion[41]. Rough mutants are more frequently isolated after a persistent infection has been established for a long period, in both CF and non-CF patients[155,156].

The smooth and rough genetic variants represent two phenotypic extremes of *Mab* physiology. However, the rough variants only form in some infections, and it is thought that most infections are established by smooth strains[41]. Smooth strains are known to form biofilms *in vitro*[44,145] and are thought to also form biofilms during infection[146]. Antibiotic-recalcitrant *Mab* infections are likely to involve mature biofilms growing in complex nutrient environments. However, *in vitro*

Mab biofilm studies have been done on immature biofilms in simple nutrient environments[44,145]: in these conditions there are modest differences in antibiotic tolerance between biofilm-associated and planktonic cells[44]. Thus, it is not clear to what extent biofilms contribute to antibiotic tolerance during infection.

In this work, I sought to determine how cell surface physiology, biofilm formation and antibiotic tolerance are affected by media conditions in *Mab* ATCC19977. I found that the cell surface, as measured by fluorescent staining, is different in *Mab* in Artificial Cystic Fibrosis Sputum (ACFS) media compared to either minimal HdB media or in the standard mycobacterial growth media, 7H9. In addition, both smooth and rough strains display more TDM in the ACFS media. When I compare biofilm and planktonic cells, I find that both populations are quite antibiotic tolerant in HdB and 7H9, while the planktonic cells are more susceptible to antibiotics in ACFS media.

3.3 Results

To determine how different nutrient conditions affect basic cell physiology, I measured growth rate and microscopically examined *Mab* in three different media. *Mab* grows fastest in 7H9 media (Fig 3.1AB), even though the Artificial Cystic Fibrosis Sputum (ACFS) media is richer[157]. *Mab* in ACFS media appears to die off more in stationary phase, implying that the nutrient richness may not prepare cells for certain stresses (Fig. 3.1A). I imaged cells using phase microscopy and observed that cell lengths were longer in ACFS media (Fig. 3.1CD). I stained log. phase cells in each media with both NADA, a 4-chloro-7-nitrobenzofurazan-conjugated D-

alanine[158], which is integrated into peptidoglycan, and FM4-64, which stains the inner membrane[159]. Although growth rates were more similar in HdB and ACFS media, cell surface staining was more similar in HdB and 7H9. The NADA staining in Hdb and 7H9 was consistent with studies performed in other mycobacterial cells: brighter staining at the septa and poles where new peptidoglycan is inserted[160]. FM4-64 stained most cells in these media types dimly, but a subset stained more brightly. Staining of cells in ACFS media was more homogeneous (Fig. 3.1DE). I observed in the phase images that cells growing in ACFS appear to be encased in translucent sheaths, which could alter access of the stains to the cell (Fig. 3.1D). These data show that *Mab* is physiologically different in typical lab media than in media that mimics the nutrient conditions in the lungs of Cystic Fibrosis patients.

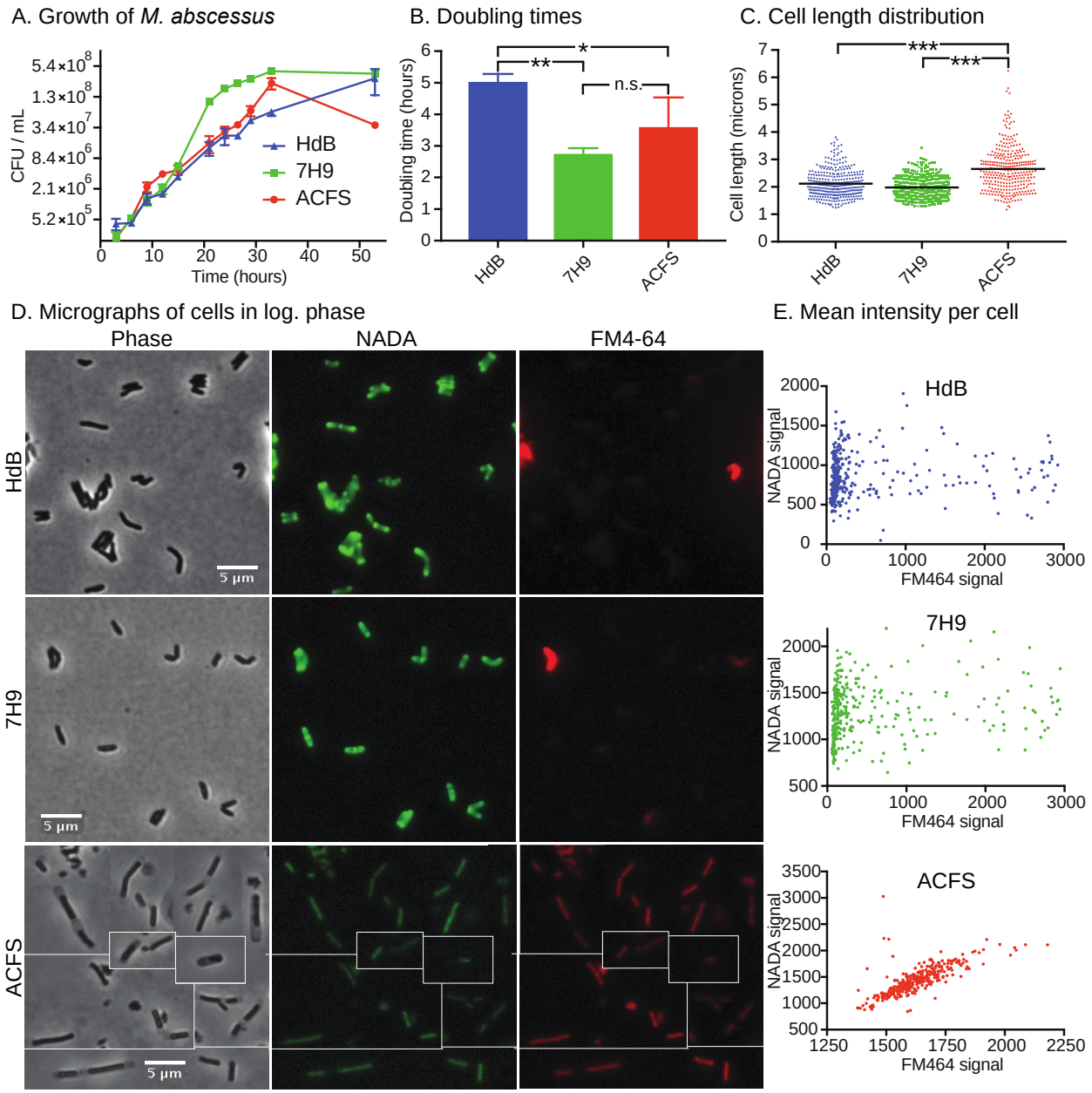

Figure 3.1. The physiology of *Mab* planktonic cells varies according to media type. A) Colony forming units over time in the three growth media on a 2-log scale. B) Maximum doubling times during log. phase growth, calculated from data in (A). P values calculated by one-way ANOVA with Tukey correction. Hdb vs. 7H9, P=0.0059; Hdb vs. ACFS, P=0.0459. C) Quantification of cell lengths of *Mab* cells in log. phase, in the three media types. At least 300

cells from two biological replicates were imaged by phase microscopy and cell lengths were calculated using MicrobeJ. ACFS vs. HdB, P<0.0001; ACFS vs. 7H9, P<0.0001. D) Micrographs of log. phase cells stained with the fluorescent D-amino acid NADA and the membrane stain FM4-64. E) Quantification of the average fluorescent intensity for at least 300 cells from two biological replicates, stained with NADA and FM4-64, as in (D).

To study the physiology of biofilms, I sought to develop a method to separate biofilm and planktonic cells from the same culture well: this allows us to control internally for nutrient depletion in the media, which also impacts cell physiology and antibiotic tolerance. I incubated standing cultures in tissue culture-treated plates. Biofilms form at the bottom of each well, while the planktonic cells remained in the media in the upper half of the well. I pipetted off all the media on the top of each well to isolate planktonic cells, then resuspended the surface-associated cells on the bottom of each well in 7H9 with Tween80, a non-ionic detergent, which broke apart cell clumps. To determine whether 7H9 + Tween80 was sufficient to break apart clumps or whether sonication was necessary, I compared the colony forming units (CFU) produced from biofilm resuspensions with and without sonication. Sonication did not change the CFU counts, so I conclude that resuspension in 7H9 + Tween80 alone is sufficient to break apart smooth *Mab* biofilms. Therefore, I used that method for biofilm enumeration in subsequent experiments.

I next analyzed how the three media types affect biofilm development and morphology. I grew *Mab* in the three different media types over time and monitored biofilm development by CFU assay and photography. Biofilms growing in all media types reach maximal cell density by day 6 (Fig. 3.2). Biofilms in ACFS form three-dimensional plumes in standing culture, while those in HdB or 7H9 are flat and almost crystalline. I did not observe pellicles in the media conditions I tested using smooth *Mab* strains (Fig. 3.2). From these data I conclude that biofilm morphology was affected by media condition.

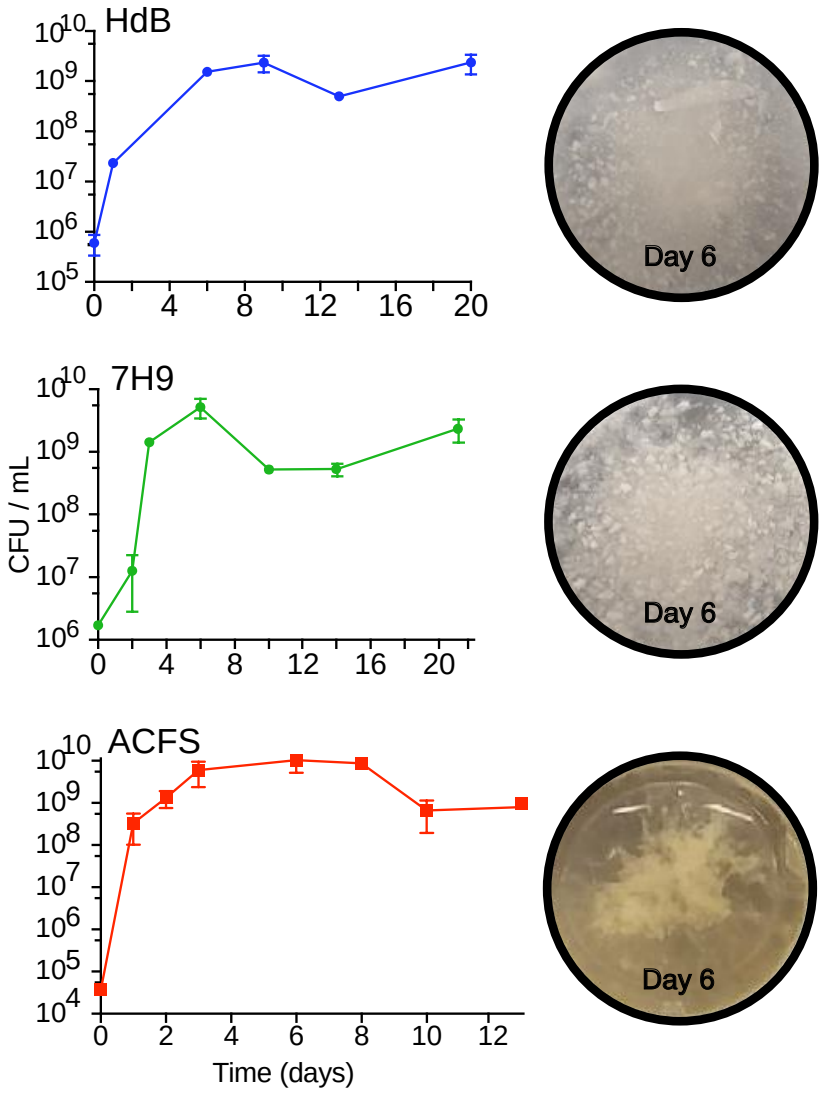

Figure 3.2. The development and macroscopic structure of *Mab* biofilms in different media. Colony forming units for biofilm-associated cells in standing culture over time. Images of corresponding wells taken at 6 days.

To probe the physiological differences between biofilm and planktonic cells in our assay, I tested their ability to respond to induction of a reporter transcriptionally and translationally. I transformed *Mab* with a plasmid that expresses Tag-RFP under the control of a constitutive P_{GroEL} promoter, and expresses eGFP under control of an inducible $P_{nitrile}$ promoter. I allowed biofilms of this culture to mature for 6 days, then induced them with isovaleronitrile to induce expression of eGFP. After 24 hours of induction, I resuspended and fixed cells from the planktonic and biofilm populations in each media type, and visualized the cells by fluorescence microscopy (Fig. 3.3A). I found that in all media conditions, cells in biofilms are less likely than planktonic cells to express significant eGFP upon induction, compared to the constitutive Tag-RFP (Fig. 3.3B). This shows that biofilm cells are either less permeable to the inducer, or are less transcriptionally and translationally active than planktonic cells in the same culture well, or both. These data also validate our method of separating planktonic cells from biofilm cells, by showing separated cell types are physiologically distinct in all three media types.

A. Micrographs of Live/Dead reporter in ACFS

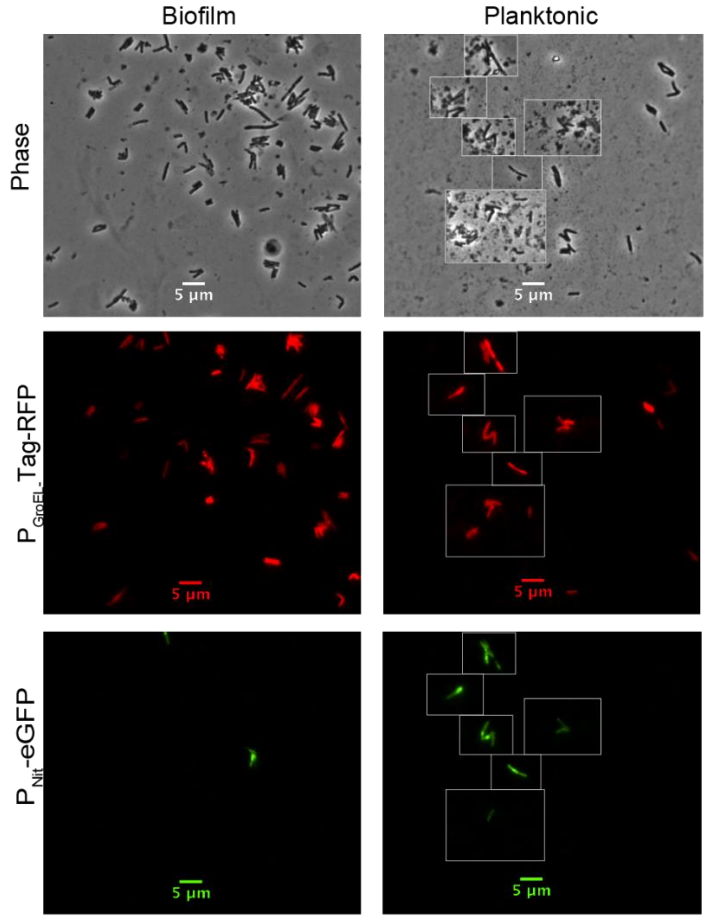

B. Percent induced in ACFS, 7H9 and HdB

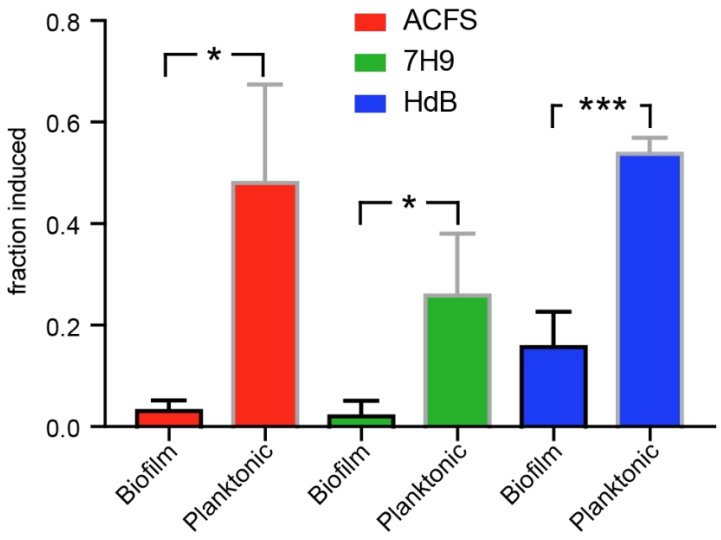

Fig. 3.3. Cells in *Mab* biofilms are less responsive to a transcriptional inducer. (A) Micrographs of *Mab* cells carrying the pDE43-MEK-Nit-live/dead vector from biofilms grown for 6 days in ACFS, then induced with 10^{-6} isovaleronitrile for one day before fixation and imaging. Living cells that retain the vector show constitutive Tag-RFP signal, inducible cells also show eGFP signal. (B) Percentage of cells with average Tag-RFP signal intensities above 400 that also have average eGFP signal intensities above 100 in each condition. At least 100 cells each from three independent biological replicates were quantified for each condition. P-value of biofilm vs. planktonic for ACFS, 7H9 and HdB medias are 0.0152, 0.0271 and 0.0007, respectively. P-values were calculated using an unpaired t-test.

Because biofilm morphology varied so greatly between media types (Fig. 3.2), I hypothesized that media could affect glycolipid expression. I extracted surface glycolipids from planktonic smooth and rough strains grown in 7H9 and ACFS (Fig. 3.4A) as well as from mature biofilms grown in all three media conditions (Fig. 3.4B). I then separated the glycolipids by thin layer chromatography (TLC). TLC analysis shows that the smooth strain expresses similar levels and types of GPLs irrespective of media condition, while the rough strain produces minimal GPLs (Fig. 3.4A). In biofilms, the smooth strain expresses GPLs in all conditions (Fig. 3.4B,D). Based on previous GPL analyses[41], the purple spot near the top (Fig. 3.4B, spot c) is an unidentified wax, while the dark purple spot at the bottom (Fig. 3.4B, spot d) is trehalose dimycolate (TDM)[161]. Both smooth and rough strains have increased TD3.M in ACFS compared to lab media, in both planktonic cultures (Fig. 3.4A) and biofilms (Fig. 3.4B). I observe a statistically significant increase in the wax (Fig. 3.4B,C) and TDM in ACFS (Fig. 3.4B,E). The levels of GPLs appear to be similar (Fig. 3.4B, D). These data show that media conditions affect the

surface glycolipid expression of *Mab* and that *Mab* grown in ACFS media has higher levels TDM, a glycolipid that is a virulence factor in *Mtb* infections[153].

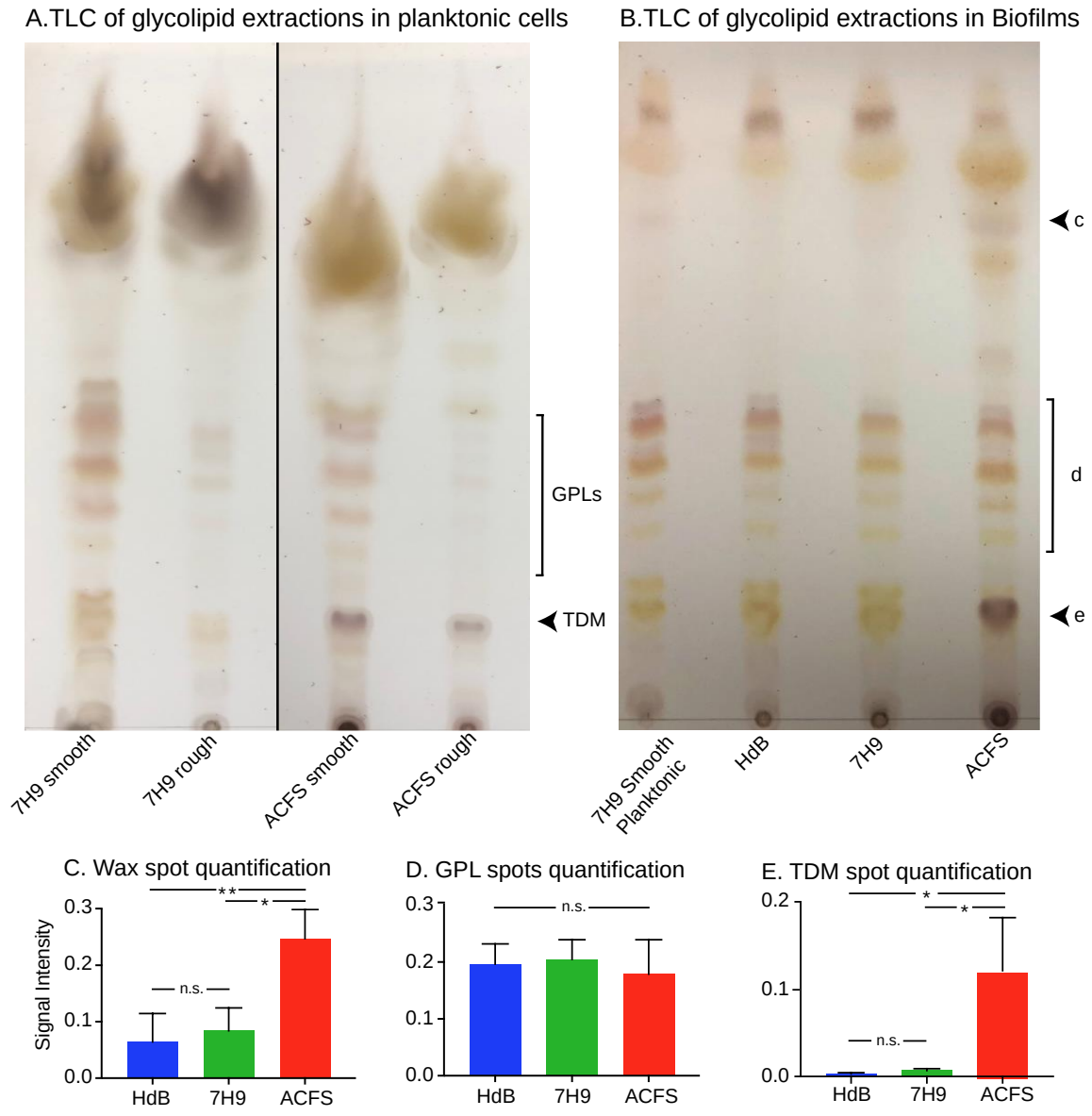

Figure 3.4. Glycolipid profiles are affected by media condition. (A) Thin Layer Chromatography (TLC) of glycolipid extractions from planktonic cultures of rough and smooth *Mab* strains grown in 7H9 and ACFS. GPLs = glycopeptidolipids, TDM= trehalose dimycolate. (B) Representative TLC of glycolipid extracts from mature biofilms of smooth *Mab* in Hdb, 7H9

and ACFS. Extraction from planktonic cells grown in 7H9 + Tween80 was used as a control sample. Black arrows indicate lipid species prominent in ACFS: c - unknown wax; d – GPLs; e - TDM. (C, D, E) Quantification of the signal intensity for each spot in (B) by means of spot densitometry. Values shown are the mean of three biological replicate experiments with error bars representing the standard deviation. (C) Wax, P-values between ACFS vs. Hdb and ACFS vs. 7H9 were 0.0079 and 0.0134, respectively. (D) GPLs, no significant differences. (E) TDM, P-values between ACFS vs. Hdb and ACFS vs. 7H9 were 0.0149 and 0.0171, respectively. P-values were calculated using one-way ANOVA with Tukey correction for multiple comparisons. Signal intensities for (D) were quantified by using the red channel only of the TLC images, to eliminate the signal from the yellow spots in the same area.

I sought to determine how biofilm maturity affects antibiotic tolerance. For these and all subsequent biofilm experiments, I compared survival of biofilm and planktonic cells from the same well of a 24-well plate for each replicate. I incubated *Mab* in ACFS media for 3, 6 or 11 days, then treated each well with two clinical drugs, clarithromycin and imipenem. I then measured survival over time and found that tolerance increases over time in standing culture, likely due to nutrient depletion of the media (Fig. 3.5AB). In 3-day and 6-day old biofilms, planktonic cells die off substantially upon treatment, while at 11 days both populations are quite tolerant (Fig 3.5A). 6-day old biofilms had higher tolerance compared to the planktonic cells in the same well at both 24 and 48 hours of treatment (Fig. 3.5B). From this, I conclude that at six days the biofilms in ACFS media are mature enough to substantially protect cells against antibiotics. Based on these results, and the fact that biofilms in all media types reached maximal

cell density at six days (Fig. 3.2), I conducted all subsequent biofilm assays with 6-day old biofilms.

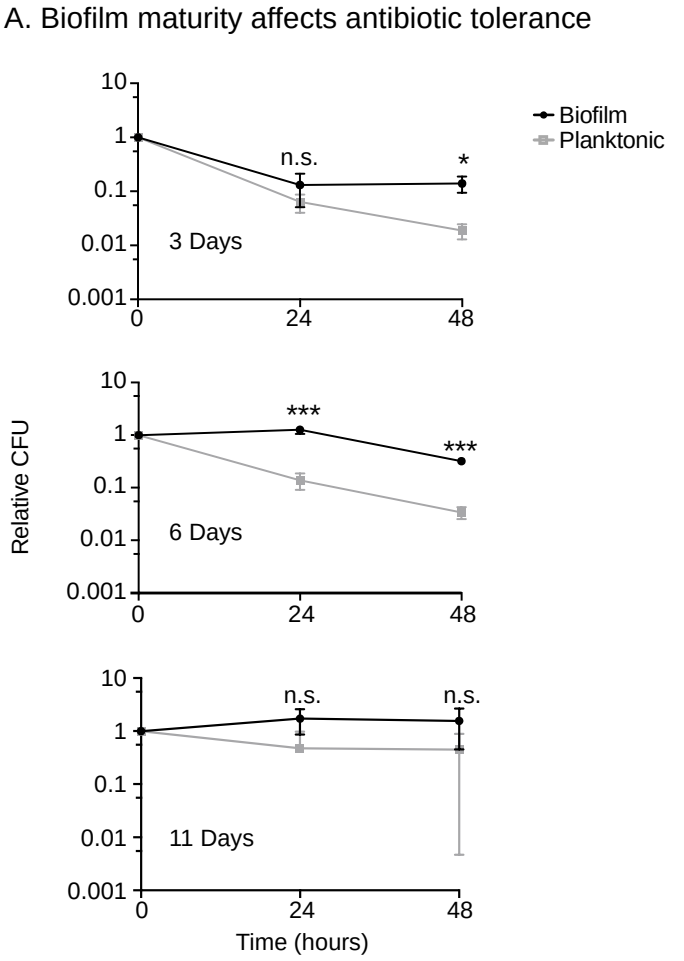

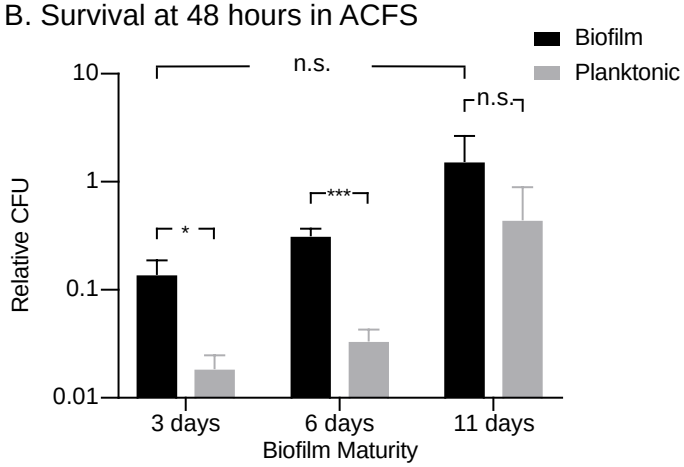

Figure 3.5. Antibiotic tolerance increases as ACFS biofilms mature. (A) Relative CFUs (CFU at each time point divided by the CFU value before treatment, *i.e.*, t=0) from biofilms and planktonic cells from the same wells, grown for 3, 6 and 11 days in ACFS. Cultures were treated with clarithromycin (20 ug/mL) and imipenem (15 ug/mL) for 48 hours, and CFUs were measured at 0, 24 and 48 hours. (B) Survival from 48-hour CFU time points (triplicate wells). P-values between biofilm and planktonic cells are 0.01099, 0.0006, 0.1815, for 3, 6, and 11 days respectively. P-value for biofilms between 3 and 11 days is 0.09046. P-values were calculated using the student's t-test.

To determine how media type affects the antibiotic tolerance of *Mab* biofilms, I treated 6-day old biofilms grown in different media types with varying concentrations of the clinically used antibiotics amikacin, clarithromycin and cefoxitin, and then plated both the biofilm and planktonic cells at 48 hours after treatment. I found that amikacin consistently killed planktonic cells at nearly an order of magnitude more than the biofilm cells from the same well, across media types. With clarithromycin and cefoxitin treatment, however, I saw much more variability. With both these antibiotics, planktonic cells and biofilm-associated cells were both highly antibiotic tolerant in both 7H9 and HdB. However, in ACFS, planktonic cells were much more sensitive to clarithromycin and cefoxitin than biofilm-associated cells. Clarithromycin was the only drug that was able to kill biofilm-associated cells at concentrations below 50 μg/ml, and this only occurred in ACFS media (Fig. 3.6).

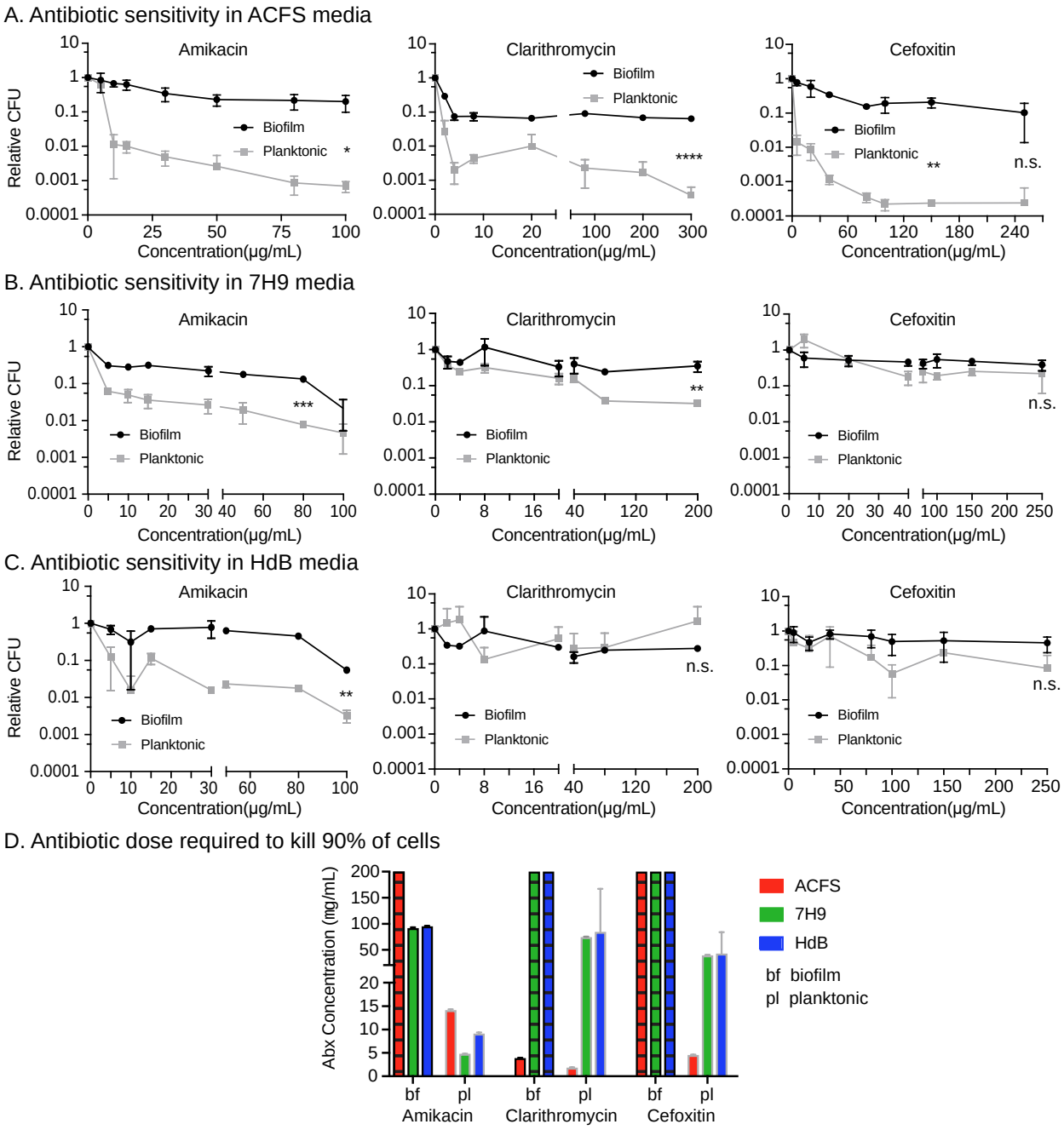

Figure 3.6. Antibiotic sensitivity varies by antibiotic and media type. (A, B, C) Relative CFUs of 6-day old biofilms and planktonic cells from the same wells after 48 hours of treatment with a range of antibiotic concentrations in 3 medias. Asterisks represent significance as measured by the student's t-test; * = $P \leq 0.05$; ** = $P \leq 0.01$; *** = $P \leq 0.001$; n.s. = $P > 0.05$. (D) LD90 (dose required to kill 90% of the cells) analysis of the data from A, B and C. Bars with

hatched lines indicate that I was unable to observe killing of 90% of the population at any concentration used, so the LD90 is above 200 μg/mL. The LD90 was calculated for each replicate and the bars indicate mean and with standard deviation.

In our assays, the biofilm-associated cells are likely to have access to less oxygen than the planktonic cells. I sought to determine whether hypoxia could differentially affect cells depending on the media. I made cultures of *Mab* in tubes with minimal headspace, sealed the tubes with septum caps, and incubated them without shaking for 13 days. I then injected cefoxitin through the caps and measured survival after 48 hours. Results show that hypoxic *Mab* exhibits tolerance in both 7H9 or ACFS media, comparable to that seen in biofilms (Fig. 3.6AB). Thus, as for *Mtb*[162], hypoxia promotes antibiotic tolerance in *Mab* and is likely to be one factor in the antibiotic tolerance seen in biofilm-associated cells.

3.4 Discussion

Bacterial physiology is enormously plastic. Bacterial cell size, shape, growth rates, surface properties and gene expression all change profoundly even between different lab media conditions[163,164]. This plasticity makes it very difficult to determine the physiological state of a pathogen during infection. In this study, I sought to physiologically profile the emerging pathogen *M. abscessus* in two standard lab growth medias and one media designed to mimic the nutrient conditions in the lungs of Cystic Fibrosis patients (ACFS). I found that, compared to standard lab medias, ACFS media induces profound physiological changes in *Mab*, both in planktonic (Fig.3.1, Fig. 3.4) and biofilm states (Fig. 3.4, Fig. 3.6).

Bacterial biofilms are complex structures which, on the macro scale, vary physiologically according to developmental stage[165], surface type[166] and nutrient conditions[167]. On the microscopic scale, there is also heterogeneity within a single biofilm: cells in different places within the biofilm express different surface factors and have different gene expression profiles[168–170]. Thus, it is not meaningful to merely compare the phenotypes of "biofilm" and "planktonic" cells from a given species, as there is enormous phenotypic variety within each of these categories. In this work, I profiled some of the phenotypic diversity possible in *Mab* biofilms in order to assess the extent to which *in vitro* biofilm experiments might be relevant to the physiology of *Mab* biofilms within the lungs of CF patients. Our results show that *Mab* biofilms in ACFS media have important physiological differences from biofilms in the standard mycobacterial lab medias HdB and 7H9 (Fig. 3.2, Fig. 3.4, Fig. 3.6). The fact that such differences can be seen even between *in vitro* media conditions shows that *Mab* biofilm physiology is responsive to environmental conditions. I hypothesize that *Mab* physiology in HdB and 7H9 media is unlikely to represent its physiology during infection. Our results do not establish ACFS media as a proxy for infection, which of course includes many host immune factors that cannot be mimicked *in vitro*. However, these data show that nutrient conditions that might be encountered by *Mab* in the host could have an important role in the pathogen's expression of virulence glycolipids and responsiveness to antibiotic treatment.

Even in experiments with the smooth *Mab*, which produces GPLs, I observed differences in the appearance of the biofilms that formed in the different media types. The biofilms in both HdB and 7H9 appeared flat and flaky, while the biofilms that formed in the ACFS media looked wet

and formed tendrilly plumes (Fig. 3.2). These differences could be merely due to the chemical and viscosity differences between the media types, or they could be due to changes in *Mab* cell physiology in the different media types. I profiled the surface glycolipids and antibiotic sensitivity of cells in these different biofilms, and found that cells in ACFS biofilms are physiologically distinct: they display more trehalose dimycolate and a non-polar wax species than biofilms in 7H9 and HdB (Fig. 3.4) and they exhibit more relative antibiotic tolerance compared to planktonic cells (Fig. 3.6).

Because nutrient availability affects the physiology of cells within a biofilm, I sought to develop methods that would allow us to disentangle responses to nutrients from responses to biofilm formation. Other groups solved this problem by moving biofilms to fresh media each day[44,145]. I assumed that nutrients would not be unlimited during infection, and so worked to assess biofilm physiology in nutrient-limited culture (Fig. 3.2, Fig. 3.5). In order to control for the well-known effects of nutrient limitation on antibiotic tolerance[171], I compared biofilm and planktonic cells from the same culture wells. These cells are sharing the same depleted nutrients, so differences in physiology should be due to association with the biofilm, or to differences in access to oxygen. While I observed considerable antibiotic tolerance in 7H9 and HdB against clarithromycin and cefoxitin, there was similar tolerance in planktonic and biofilm-associated cells (Fig. 3.6B,C), even though the planktonic cells presumably have more access to oxygen at the top of the well. This implies that antibiotic tolerance in these media conditions is due to some other environmental factor, such as nutrient depletion, rather than due to the protection of the biofilm or to hypoxia. In the more nutrient-rich ACFS media however, I see much higher sensitivity to cefoxitin and clarithromycin in the planktonic cells, while the biofilm-associated cells are

tolerant. Therefore, the physiological difference between biofilm and planktonic cells is greater in ACFS media than in typical lab medias.

Our results imply that the modest degree of antibiotic tolerance in biofilms that has been observed before[44] may be a function of the culture conditions. Our data show that mature biofilms grown in ACFS media afford considerable protection against three clinical antibiotics from different classes. While the ACFS media may mimic the nutrient conditions of sputum, it does not replicate a complex host environment with active immune cells and tissue structures, so the physiological state of *Mab* in a true infection remains unknown. However, our results imply, during infection in CF patients, *Mab* may express more of the virulence glycolipid TDM, and be more antibiotic tolerance that experiments in regular lab media might indicate. Thus, treatments that could help disrupt *Mab* biofilms or prevent their establishment could help clear these infections more quickly. A deeper understanding of the chemistry and genetics of biofilm formation and physiological responses in *M. abscessus* will be needed in order to determine the role of biofilms in infection and treatment recalcitrance and to develop better treatment protocols.

3.6 Materials and Methods

3.6.1 Media and culture conditions. All *M. abscessus* ATCC19977 cultures were started in 7H9 (Becton-Dickinson, Frankin Lakes, NJ) media with 5 g/l bovine serum albumin, 2g/l dextrose, 0.85 g/l NaCl, 0.003 g/l catalase, 0.2% glycerol and 0.05% Tween80 and shaken overnight at 37C until in log. phase. All *Mab* CFUs were performed by plating serial dilutions on LB Lennox agar. Three media types varying in nutrient richness were used for all biofilm assays: Tween80 was not added to any media for biofilm assay. Hartmans de Bont (HdB) Minimal Media was made as described[136], 7H9 for biofilms was made as above, without the Tween80.

3.6.2 Artificial Cystic Fibrosis Sputum. Two protocols were combined in order to make our ACFS media[157,172]. In 500mL of ultrapure water, the unique components that comprise CF sputum were added as described[172]; 5 g of porcine mucin (NBS Biologicals), 4 g of Deoxyribonucleic Acid (Spectrum Chemicals), 5.9 mg diethylene triamine pentaacetic acid (DTPA), 5 g NaCl, 2.2 g KCl, and 1.81 g Tris base. Amino acid stocks were prepared as described[157] and stored at 4C. Except for tryptophan, amino acids were added to the media. The ACFS media was adjusted to a pH of 7, filled-up to one liter, and autoclaved at 110C for 15 minutes. The media was cooled down at room temperature prior to adding tryptophan and 5 mL of egg yolk emulsion (Dalynn Biologicals). ACFS Media was stored at 4C.

3.6.3 Biofilm assays. Log. phase biological replication cultures of *Mab* cultures in 7H9 were inoculated into tissue-culture treated 24-well plates with 2mL of the appropriate media to a final optical density of 0.02. Sufficient wells were inoculated in order to have biological triplicates for

each time point or concentration in the assay. Prior to incubation, each plate was covered with a Breathe-Easy sealing membrane (Electron Microscopy Sciences) to allow air exchange and reduce evaporation. Standing biofilm plates were incubated at 37C. The Breathe-Easy membrane was removed after biofilm development in order to add antibiotics. The biofilm plates were then re-sealed and incubated again at 37C for 24 or 48 hours. For each data point, cells from biological replicate wells were used to plate for CFU calculations. To enumerate the planktonic cells, the supernatant was extracted from each well without disturbing the biofilm and plated. The remaining biofilm was then re-suspended in 7H9 + Tween80 and serial dilutions were plated and incubated at 37°C for 4 days. Serial dilutions were done in 96-well plates in HdB + Tween80 and plated on plain LB Agar plates. Relative CFU is the ratio between each CFU value and the initial CFU value at t=0 or concentration=0.

3.6.4 Hypoxia Assay. *Mab* was grown in 7H9 until log-phase. In order to promote hypoxia, sterile glass tubes were filled near full (9 mL) with 7H9 and ACFS respectively. All tubes were inoculated to an optical density of 0.02, capped with a sterile rubber septum, and wrapped with parafilm to avoid uncapping. To establish growth cessation, standing tubes were incubated at 37C and CFUs were taken every couple days on biological replicates. Once we established that growth cessation happens at 13 days, new tubes were inoculated and incubated for 13 days. In order to avoid oxygenation, replicates were treated by injecting through the rubber septum with 80 ug/mL of cefoxitin. CFUs were taken upon addition of antibiotic (t=0), and 48 hours post-treatment. All time-points were plated on LB Agar and incubated for 4 days.

3.6.5 Glycolipid extractions and Thin layer chromatography. Mature biofilms and planktonic cultures were used for glycolipid extractions. GPLs were extracted as described[173] and spotted on TLC Silica Gel 60 plates (Millipore Sigma). In short, cells were isolated and centrifuged. Pellets were resuspended for lipid extraction in 10mL chloroform/methanol (2:1). Extractions were done twice at room temperature for 24 hours and then centrifuged at 5000rpm for 30 minutes to collect organic supernatant. Organic samples (Lipids) were evaporated with nitrogen and resuspended in 1mL chloroform/methanol (2:1) and treated with equal volume 0.2M NaOH (in methanol). Lipids were incubated at 37C for 30 minutes and then neutralized with a few drops of glacial acetic acid. Solvents were evaporated and the lipids were resuspended with 4mL of choloroform, 2mL of methanol, and 1mL of water in each tube. Samples were mixed and then centrifuged at 5000 rpm for 10 minutes to collect the organic layer. The solvent was evaporated and the remaining lipids were resuspended in 100uL of chloroform/methanol (2:1) and spotted. TLCs were developed in chloroform/ methanol/ water (100:14:0.8) as described (24). Plates were visualized with 10% Sulfuric Acid (in ethanol) and baked for 20 minutes at 120C. The signal intensity of spots was analyzed and quantified using ImageJ software by means of spot densitometry. For spot d (TDM) the TLC image was split into single color channels and quantified by measuring the signal intensity from the red channel only. Each spot intensity value was normalized against all the spots in a lane (entire lane; all in triplicates). We re-ran the TLCs, when necessary, so that total lane spot intensities were similar between samples.

3.6.6 Cell staining. For experiments on log. phase cells, *Mab* was stained with 3□L/mL of 10 mM NADA and incubated at room temperature for 15 minutes in growth media. Cells were then pelleted and resuspended in PBS+Tween80 and FM4-64 was added to a final concentration of 4

ng/mL and incubated at room temperature for 5 minutes. Cells were then fixed with 2% paraformaldehyde for one hour at room temperature, and washed and resuspended in PBS+Tween80 for imaging.

3.6.7 Microscopy. *Mab* cells were resuspended as described for plating of planktonic and biofilm cells, then fixed with 4% paraformaldehyde in PBS at room temperature for 2 hours. Cells were immobilized on agarose pads and imaged using a Nikon Ti-2 widefield epifluorescence microscope with a Photometrics Prime 95B camera and a Plan Apo 100X, 1.45 NA objective. Green fluorescent images were taken using a filter cube with a 470/40 nm excitation filter and a 525/50nm emission filter. Red fluorescent images were taken using a filter cube with a 560/40nm excitation filter and a 630/70 emission filter. Images were captured using NIS Elements software and analyzed using FIJI and MicrobeJ[174] (45).

Chapter 4 - Elucidating the Role of the CwlM-MurA Interaction in Mycobacterial Cell Wall Regulation

Augusto Cesar Hunt-Serracin[1], Karen Tembiwa[1], Arinze Awagu[1], Soroush Ghaffari[1], Katie Kang[2], and Cara Boutte[1*]

[1]Department of Biology, University of Texas Arlington

[2]Department of Immunology, UT Southwestern Medical Center

[*]Corresponding author: cara.boutte@uta.edu

4.1 Abstract

The respiratory disease tuberculosis, caused by *Mycobacterium tuberculosis*, remains a significant global health concern due to the pathogen's resilience and the challenges in treatment. The regulation of the mycobacterial cell wall, particularly the peptidoglycan layer, plays a crucial role in mycobacterial survival and antibiotic resistance during infection. Here, I investigate the interaction between the cytoplasmic amidase CwlM and the peptidoglycan precursor synthesis enzyme MurA, shedding light on its significance in mycobacterial physiology. Through computational predictions and biochemical assays, I identify a charged interaction interface between CwlM and MurA, with specific residues mediating this interaction. Mutations in this interface impair MurA activation, emphasizing its functional relevance. Importantly, while phosphorylation of CwlM is necessary for interaction, it alone is insufficient for full MurA activation, indicating complex regulatory mechanisms. Furthermore, *in vitro* assays suggest a weak interaction, highlighting potential dynamics *in vivo*. Genetic studies in *Mycobacterium*

smegmatis strains reveal that mutations affecting MurA activation led to defects in peptidoglycan metabolism, particularly pronounced with disruptions in the predicted interaction interface. These findings highlight the importance of the CwlM-MurA interaction in bacterial cell wall synthesis and offer insights into regulatory networks governing peptidoglycan metabolism, with implications for antimicrobial strategies targeting essential bacterial pathways.

4.2 Introduction

Mycobacterium tuberculosis (*Mtb*) is an obligate human pathogen and the causative agent of the lung disease Tuberculosis (TB)[9]. This disease affects millions of individuals worldwide due to *Mtb's* success as a pathogen and years of co-evolution with humans[52,175]. Despite modern medicine, a severe *Mtb* infection is challenging to treat due to the bacterium's stress response strategies and poor patient compliance during rigorous and prolonged drug treatments[176,177]. A key factor in *Mtb* pathogenesis is its waxy and armor-like cell envelope, which is known to contributes to its recalcitrance to antibiotic treatment [178]. The cell envelope of mycobacteria consist of a plasma membrane, a lipid-rich cell wall core, and other free lipids, which provide *Mtb* with shape, rigidity, hydrophobicity, and protection from outside stressors like antibiotics[47,178–180].

Although the mycobacterial cell wall structure was well-defined in the latter half of the 20th century, there is still more to be known about its regulation[181–183]. Beyond the plasma membrane, the peptidoglycan (PG) layer forms a mesh-like structure in the periplasm, providing shape and protection from osmotic stress[184]. The PG layer is covalently attached to polysaccharides known as arabinogalactan, which, along with Mycolic acids (outer membrane fatty acids), contribute to

the cell's waxy coat[185,186]. This intricate arrangement of layers forms a highly complex mycobacterial cell wall, the regulation of which is a crucial defense mechanism against environmental stress. Therefore, a comprehensive understanding of this regulation is a cornerstone in the quest for more effective therapies against drug-tolerant mycobacteria.

The synthesis and regulation of the PG layer is an involved process that begins in the cell's cytoplasm with the formation of the cell wall intermediate Lipid II[185]. It starts with the sugar nucleotide UDP-GlcNAc, and its modification into forming Lipid II by several Mur family of enzymes[179]. Because PG metabolism involves multiple steps, many PG enzymes and their regulators work tightly together to ensure cell growth occurs without compromising the cell's integrity. One example is MurA, the first enzyme in the PG precursor synthesis pathway, which is activated by the cytoplasmic amidase CwlM[58,59].

In nearly all bacteria, except wall-less forms of bacteria, MurA catalyzes the first step of PG precursor synthesis and is essential for survival[187–190]. The MurA structure and enzymatic activity have been well established in gram-negative bacteria, primarily in *Escherichia coli* (*E.coli*) and *Enterobacter cloacae*. Other bacteria like *Staphylococcus aureus*, *Enterococcus faecelis*, and *Streptococcus pneumoniae* have two copies of MurA, where the second is often called MurZ, MurA2 or MurAB. The mechanism of this second enzyme has yet to be fully understood, and it seldom can compensate for the activity of the primary MurA[191]. In either case, these proteins are involved in normal growth, making them ideal drug targets. Although inhibitors such as fosfomycin have shown efficacy against MurA in other species, changes in a key amino acid residue in *Mtb's* MurA have made this inhibitor ineffective[192].

Although MurA transferase activity is conserved across bacteria, its regulation must still be studied in several species. In *Listeria monocytogenes* and *Bacillus subtilis*, MurA activity is regulated through its degradation by the protease ClpC when bacterial growth arrest is needed[193,194]. In *Listeria monocytogenes*, phosphorylated Reom, a cytoplasmic protein, interacts with MurA to deter degradation by ClpC[193]. This result highlights the importance of MurA being the first enzyme in PG synthesis, as it controls the fluidity throughout the PG precursor synthesis pathway. In mycobacteria, in-depth biochemical studies show that MurA enzymatic activity as a PG transferase is conserved in both Mtb and the non-pathogenic relative *Mycobacterium smegmatis* (*Msmeg*)[189]. Other studies focused on MurA's relationship with the cytoplasmic amidase CwlM, which, when phosphorylated, activates MurA's enzymatic activity[58]. This study also found that CwlM is less phosphorylated during starvation, which correlates with MurA's decreased activity during growth arrest.

In this work, I analyzed the interaction site between CwlM and MurA and the effects of MurA misregulation on mycobacterial cell physiology. I ran a prediction of a CwlM-MurA interaction through AlphaFold2 Multimer, and identified a possible interaction site (Fig.5.1). I made mutants of CwlM that are predicted not to interact with MurA, which show a decrease in activation of MurA *in vitro*. Our protein interaction experiments with MurA and CwlM suggest that the interaction between these proteins is transient and weak. Lastly, in *in vivo* experiments in *M. smegmatis*, I found that ablation of the predicted interaction site did not allow cell survival, while milder mutations caused a decrease of PG metabolism *in vivo.*

4.3 Results

4.3.1 AlphaFold predicts a charged interaction interface between CwlM and MurA.

Phosphorylated CwlM, CwlM~P, activates MurA *in vitro,* and co-immunoprecipitates with MurA from cell lysates [195], suggesting that the two proteins interact. To identify a possible interaction site, I ran a AlphaFold2 Multimer[196] prediction of $CwlM_{Mtb}$ and $CwlM_{Mtb}$ - $MurA_{Mtb}$ hetero-dimer (Fig.4.1B, 4.1C). The predicted dimer shows a highly charged interaction interface (Fig. 4.1C) at an alpha-helix on $CwlM_{Mtb}$ I named "REEEL" due to the amino acid sequence, and a beta-sheet on $MurA_{Mtb}$. Glutamates 178 and 179 from $CwlM_{Mtb}$ are predicted to interact with arginines 346 and 355 of $MurA_{Mtb}$ (Fig. 4.1D).

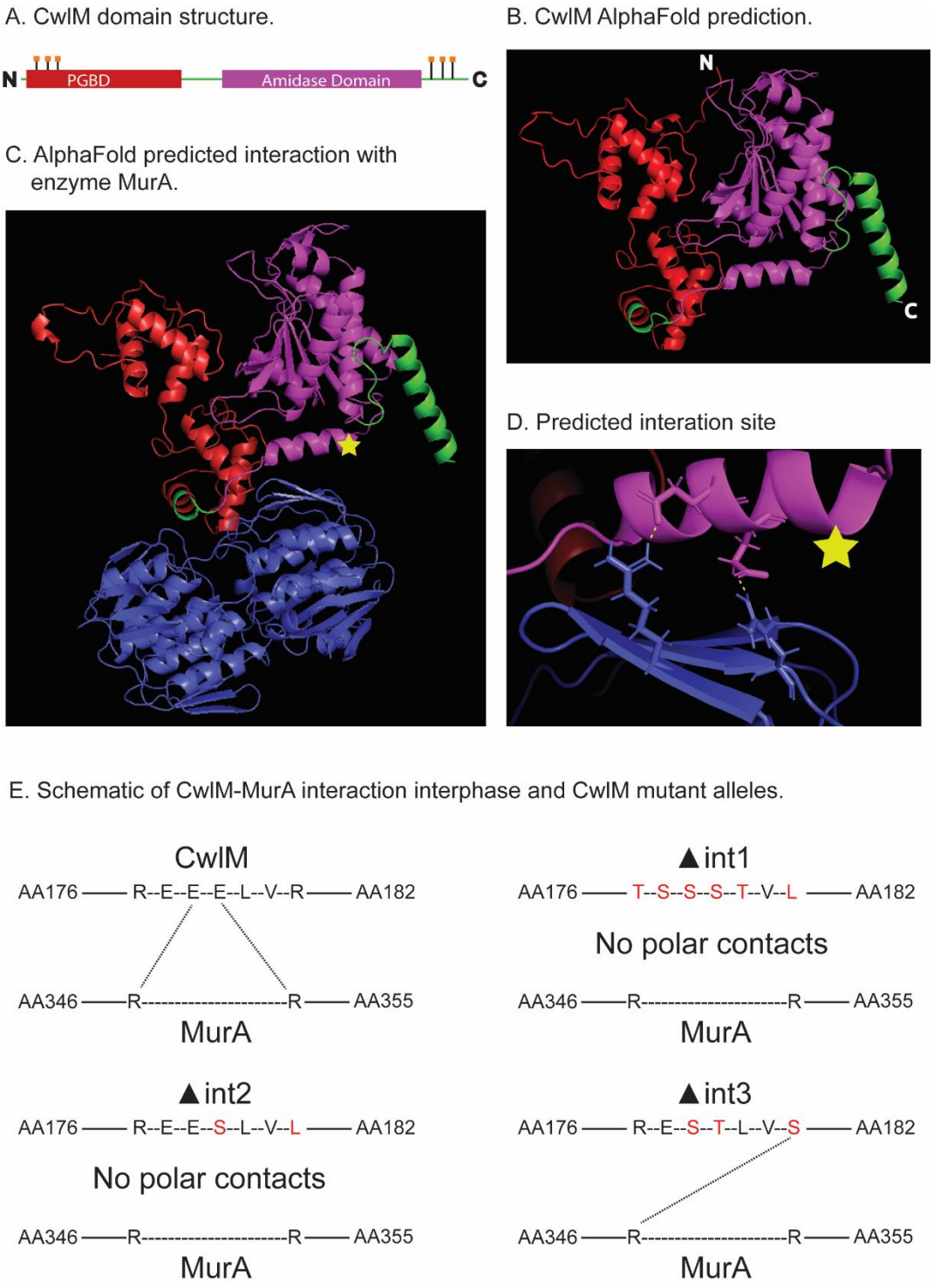

Figure 4.1 - AlphaFold prediction of CwlM-MurA interaction complex and schematic of CwlM mutants with predicted polar contacts.

4.3.2 Salt-bridges between CwlM and MurA are vital for MurA enzymatic activity.

To test how the predicted interaction impacts activation of MurA, I expressed and purified CwlM with three different sets of mutations in the REEEL region (Fig. 4.1E).

Previous experiments show that unphosphorylated CwlM has poor activation of MurA during a MurA enzymatic assay[195]. We measured MurA product formation through HPLC after incubation with substrates and wild-type or mutated CwlM, in both phosphorylated and unphosphorylated states. The HPLC traces for the wild-type CwlM$_{Mtb}$ showed the effects of phosphorylation on the activation of MurA$_{Mtb}$ (Fig. 4.2A). In both traces, CwlM and CwlM~P, I see a significant signal for the unused substrate UDP-GlcNAc, but only for CwlM~P do I see a smaller signal for the product, EP-UDP-GlcNAc (Fig. 4.2A). As a negative control, I tested a C-terminal truncation of CwlM$_{Mtb}$, which has reduced activation of MurA[195]. Compared to CwlM~P, all mutants were significantly impaired in MurA activation, regardless of phosphorylation (Fig. 4.2B). The phosphorylated CwlM mutants all activated MurA to the same degree as non-phosphorylated CwlM. I conclude that the REEEL interaction site on CwlM is necessary for the activation of MurA$_{Mtb}$, and that phosphorylation alone is not enough to rescue the activation.

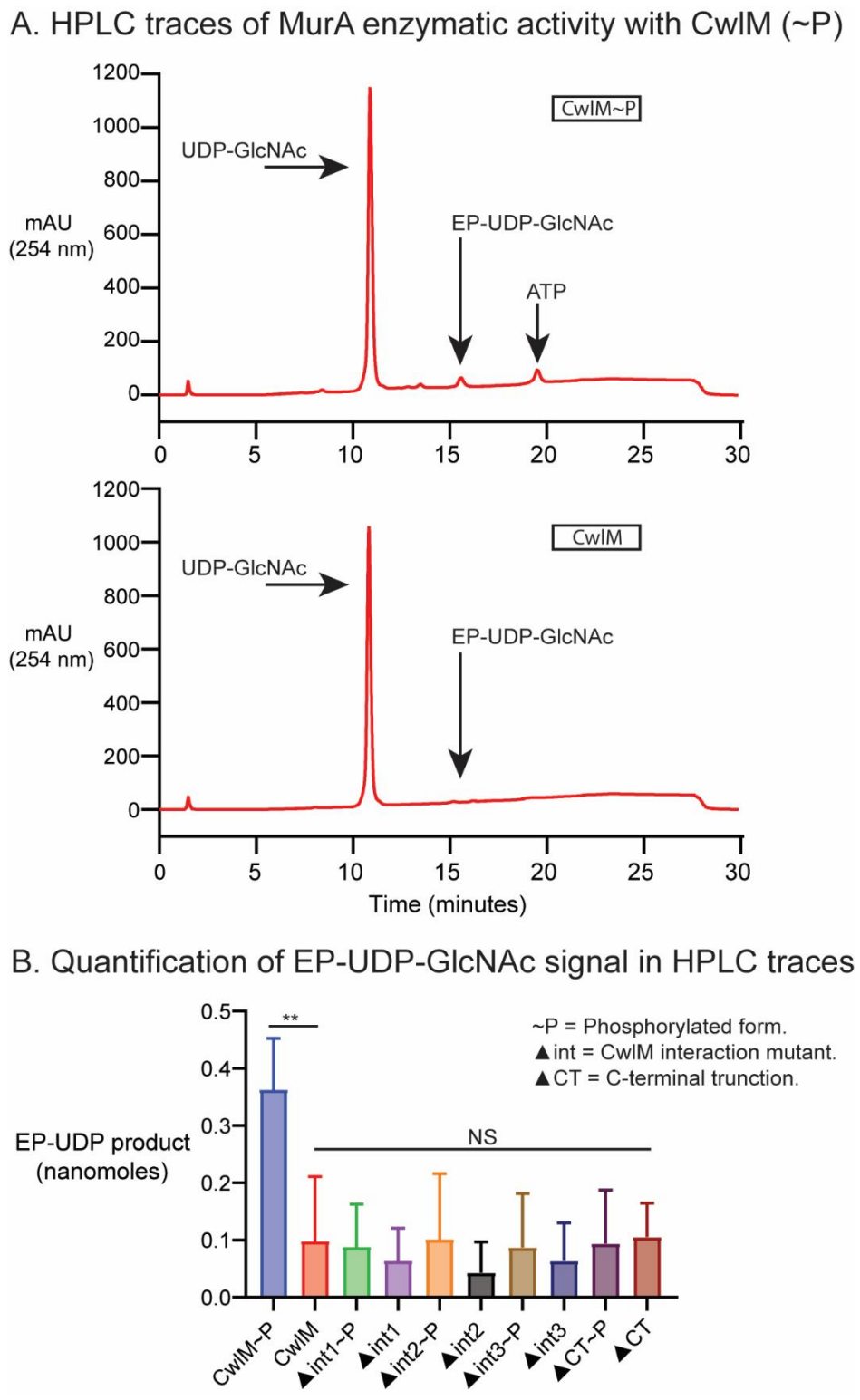

Figure 4.2 - HPLC traces and product quantification of MurA enzymatic activity.

4.3.3 The CwlM - MurA interaction is weak and difficult to elucidate through Co-immunoprecipitation type assay.

HPLC results showed the importance of the predicted interaction interface between CwlM and MurA. However, despite a reduction in MurA activity, the effects of these mutants on MurA interaction are still unclear.

Previous pulldown assays showed that a genetically FLAG-tagged CwlM could be co-immunoprecipitated through strep-tagged beads only in the presence of MurA-strep, suggesting an interaction between the two proteins[195]. I tested if I could observe this interaction with purified proteins, without cross-linking. I immobilized His-MurA$_{Mtb}$-strep on magnetic beads and poured over equimolar CwlM$_{Mtb}$ or CwlM$_{Mtb}$~P. I eluted the proteins from the strep magnetic beads, and found that both CwlM$_{Mtb}$ and CwlM$_{Mtb}$~P interact with MurA$_{Mtb}$ (Fig. 4.3). A control sample also shows that both CwlM$_{Mtb}$ and CwlM$_{Mtb}$~P can interact with the strep beads alone, but upon subtracting the control from the experimental samples I found little difference between both phospho-forms of CwlM$_{Mtb}$ and their interaction with MurA$_{Mtb}$. These results suggest that the interaction between MurA and CwlM is transient or very weak under *in vitro* experimental conditions.

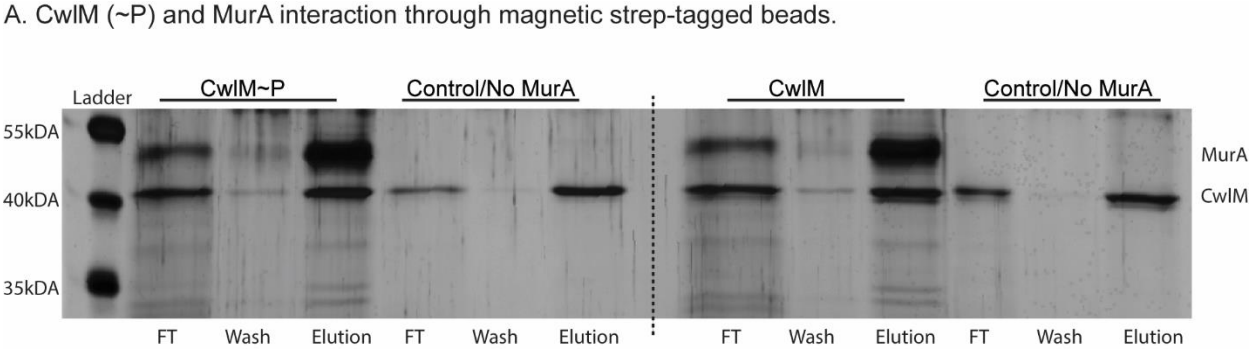

Figure 4.3 – CwlM-MurA interaction through Co-immunoprecipitation type assay.

4.3.4 CwlM interaction mutants have similar growth rates but show a decrease in peptidoglycan metabolism and transformation efficiency.

I sought to determine how the *cwlM* mutants with decreased activation of MurA *in vitro* would affect cell physiology. I built strains of *Msmeg* carrying wild-type and interaction mutant alleles of *cwlM*, in genetic backgrounds with either wild-type *murA* or *murA* S368P, in order to separate *cwlM* phenotypes that are connected to MurA activity from *cwlM* phenotypes due to other possible functions of CwlM[195]. MurA S368P is hyperactive, so mutants of *cwlM* that are specifically defective in MurA activation should have reduced phenotypic defects in this genetic background.

I started first by scoring the efficiency with which different alleles of *cwlM* exchange in L5 phage integrase allele swapping[195]. The swapping efficiency was higher in the MurA S368P background than in the MurA background in wild-type, for ▲int2 and ▲int3 alleles of *cwlM*, which have more conservating mutations in the putative MurA interaction site. But for ▲int1, containing six amino acid mutations in the REEEL site (Fig. 4.1E), there was no recovery in either MurA background (Fig. 4.4A). The ▲int1 results suggest that abrogation of the charged residues at this site either completely prevents MurA activation, or has a detrimental effect on other functions of CwlM besides the activation of MurA. To verify that these results were not due to protein folding, I performed western blots on merodiploid strains containing wild-type $CwlM_{Msmeg}$ in the native site and the different $CwlM_{Msmeg}$ mutants at the L5 integration site.

Results showed that all CwlM$_{Msmeg}$ mutants had no difference in protein stability compared to the wild-type (Fig. 4.4B).

To test whether the CwlM mutants had any growth defects under normal growth conditions, I performed growth curves. Despite differing in MurA activation and swapping efficiency (Fig 4.2B, 4.4A), Strains with *cwlM*▲int2 and ▲int3 had the same doubling time as wild-type *cwlM*$_{Msmeg}$ regardless of *murA* background, suggesting that these mutations have little effect on growth rate (Fig. 4.4C).

Since MurA is the first enzyme in peptidoglycan precursor synthesis, I hypothesized the strains with *cwlM* alleles that are defective in MurA activation could alter peptidoglycan metabolism. To address this, I grew our strains with different *cwlM* and *murA* alleles to log. phase and stained them with HADA, a fluorescent D-amino acid[197]. Results from imaging showed decreased HADA signal in strains with *cwlM*▲int2 and ▲int3 compared to *cwlM* wild-type in the wild-type *murA* background. In contrast, only *cwlM*▲int2 shows a significant defect in the *murA* S368P background (Fig. 4.4D). I find that HADA staining helps validate the importance of the predicted polar contacts between CwlM and MurA.

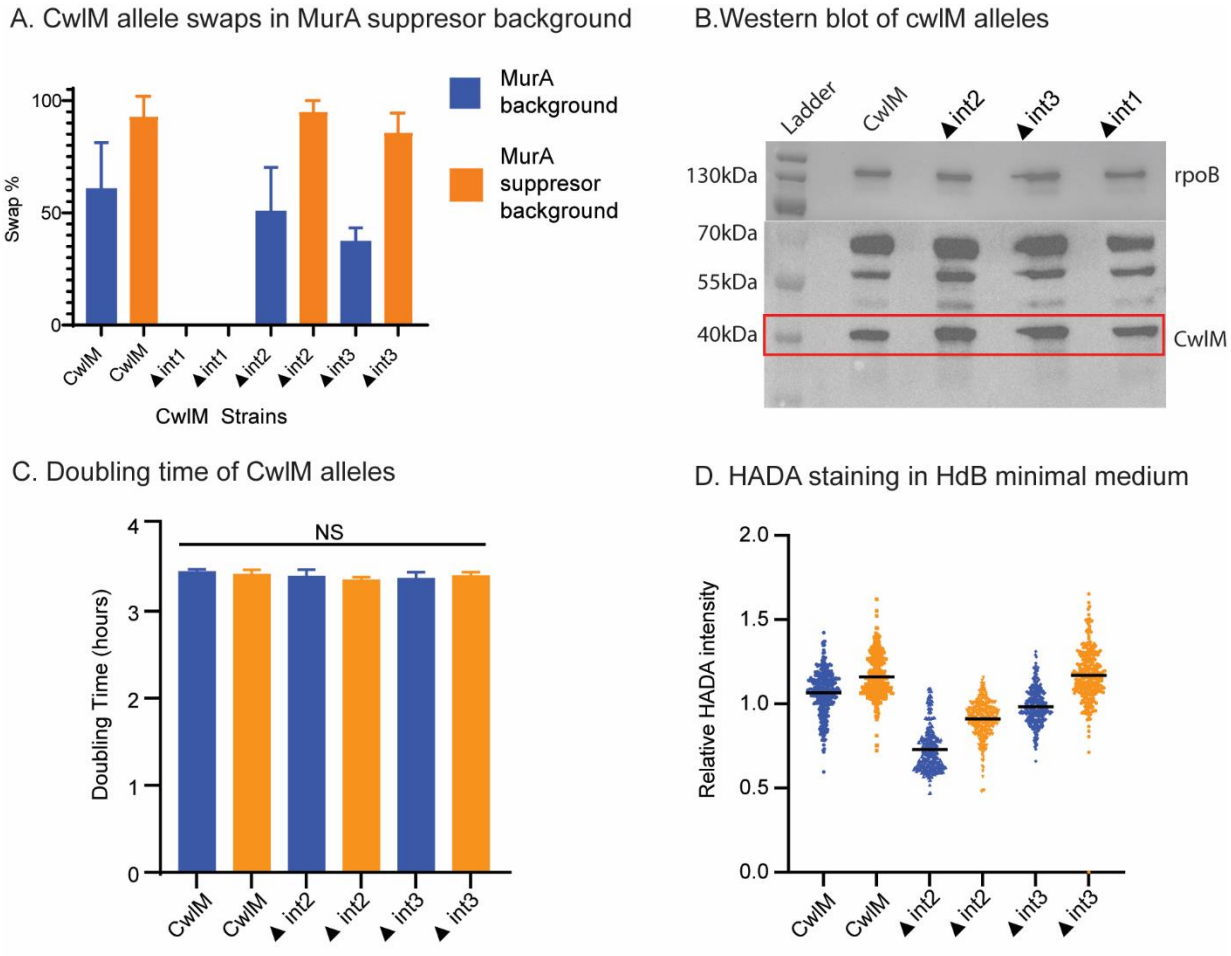

Figure 4.4 – Effects of *cwlM* alleles on mycobacterial cell physiology.

4.4 Discussion

The basis of our experiments arise from prior research on CwlM, a cytoplasmic peptidoglycan amidase (Fig. 4.1A), which when phosphorylated by the kinase PknB, activates MurA, an enzyme involved in the first step of peptidoglycan precursor synthesis[195]. The results presented here shed light on the interaction between CwlM and MurA and its significance in bacterial physiology, particularly in the context of cell wall regulation of the peptidoglycan layer of mycobacteria. Through a combination of computational predictions, biochemical assays, and genetic manipulations, I have elucidated key aspects of this interaction and some implications in cellular function.

Using AlphaFold2 I predicted a charged interaction interface between CwlM and MurA, with specific residues identified as potential mediators of this interaction complex (Fig. 4.1B, 4.1C). These ionizable residues would form salt-bridges between CwlM and MurA, allowing a close interaction between the two proteins (Fig. 4.1D, 4.1E). Salt bridges are known to provide stability within and between proteins, as well as an important role in protein-protein interaction and regulation[198]. This predicted interaction was first studied through biochemical assays, which demonstrated physical interaction between CwlM and MurA *in vitro*, and its importance for MurA enzymatic activity (Fig. 4.2). Specifically, mutations in the predicted interaction site on CwlM, termed "REEEL," led to a significant impairment in MurA activation, highlighting the functional relevance of this interaction interface. Interestingly, our data suggest that while phosphorylation of CwlM is important for its interaction with MurA, phosphorylation alone is insufficient to rescue MurA activation fully. This underscores the complex regulatory mechanisms governing the CwlM-MurA interaction and suggests the involvement of additional factors or modifications in modulating their functional interplay. I theorize that CwlM and MurA

experience a regulatory interaction, in which phosphorylated CwlM can stabilize MurA in the ideal conformation through the REEEL site, encouraging optimal enzymatic activity.

Furthermore, our findings indicate that the CwlM-MurA interaction is transient or weak under *in vitro* conditions (Fig. 4.3), which may have implications for understanding the dynamics of peptidoglycan biosynthesis *in vivo*. To dissect the physiological consequences of perturbing the CwlM-MurA interaction, I employed genetic approaches using *Mycobacterium smegmatis* strains harboring wild-type and mutant alleles of *cwlM* and *murA* (Fig. 4.4). Our results demonstrate that mutations affecting MurA activation led to defects in peptidoglycan metabolism, as evidenced by reduced fluorescence intensity upon staining with the D-amino acid analog HADA. Importantly, these defects were more pronounced in strains with cwlM mutations that disrupted the predicted interaction interface, further supporting the functional relevance of the CwlM-MurA interaction in bacterial cell wall synthesis.

Overall, our findings provide novel insights into the molecular mechanisms underlying peptidoglycan metabolism and highlight the importance of protein-protein interactions in bacterial physiology. Further studies elucidating the regulatory networks governing the CwlM-MurA interaction and its impact on cell wall biosynthesis may offer new avenues for the development of antimicrobial strategies targeting essential bacterial pathways.

4.6 Materials and Methods

4.6.1 AlphaFold predictions. AlphaFold is a protein structure prediction tool developed by DeepMind (Google)[1], which uses primary sequences to predict 3D protein structures. Protein sequences for both *MSMEG* and *Mtb* proteins were sourced from Mycobrowser.epfl.ch website.

AlphaFold monomer and multimer predictions were performed at the Texas Advanced Computing Center (TACC) at the University of Texas at Austin. Sequences were submitted remotely through Windows PowerShell and ran on TACC's Lonestar6 High Performance Computer system. For more information, visit tacc.utexas.edu.

4.6.2 Media and culture conditions. All *E.coli* cultures were started with Luria-Bertani (LB) medium and shaken overnight at 37C. All *MSMEG* MC^2155 wild-type and mutant cultures were started in 7H9 (Becton, Dickinson, Franklin Lakes, NJ) medium with 5 g/liter bovine serum albumin, 2 g/liter dextrose, 0.85 g/liter NaCl, 0.003 g/liter catalase, 0.2% glycerol, and 0.05% Tween 80 and shaken overnight at 37° C until cultures entered logarithmic phase. For starvation and other specific assays, Phosphate buffer saline (PBS) and Hartmans-de Bont (HdB) minimal medium was made as described previously[2,3]. Cultures were inoculated to OD_{600} 0.05, unless otherwise stated. All CFU time points were plated on LB agar, and placed in 37° C incubator for 3-4 days.

4.6.3 Protein expression and purification. All proteins were expressed using *E.coli* BL21 codon plus cells. Starter cultures were inoculated in 150 mL of LB medium, then incubated overnight at 37C with the appropriate antibiotic. The following day 1 liter LB cultures were inoculated to an OD of 0.2, and shaken at 37C until OD 0.8. Cultures were then submitted to cold-shock for 30 minutes, prior to induction. N-terminal tagged His-$MurA_{Mtb}$ cultures were expressed for 4 hours with 1mM of isopropyl-B-D-thiogalactopyranoside (IPTG). The 1-liter cultures were then pelleted down at 4,000 rpm for 20 minutes, and then resuspended with cold MurA lysis/wash buffer (50m Bis-Tris propane pH 7.5, 500mM NaCl, 2mM TCEP, 5 mM Imidazole, 10% glycerol).

Resuspended cells were then lysed using the Emulsiflex C-5 instrument (AVESTIN). Lysates were then pelleted at 35,000 x g for 35 minutes at 4C. Supernatants were filtered then poured over Ni-NTA resin column (Econofit Nuvia IMAC #12009287). Nickel bound proteins were then washed and eluted with MurA buffer containing 5 mM and 500 mM Imidazole, respectively. Elution fractions were concentrated and soluble proteins were separated from aggregates through a Sephacryl S-200 resin (Cytiva) filled column (GE Healthcare XK 26/70) in MurA SEC buffer (MurA wash buffer with no Imidazole). Soluble proteins were concentrated and stored in 20% glycerol. N-terminal tagged His-SUMO-CwlM*Mtb* and His-SUMO-CwlM*Mtb* mutants were harvested and purified similarly as His-MurA*Mtb*. In short, CwlM*Mtb* was induced for 18h overnight at 18 C with 1mM IPTG. CwlM buffer consisted of 50 mM Tris pH 7.5, 350 mM NaCl, 1 mM DTT, 10% glycerol, and Imidazole (10mM wash, 250mM elution, no imidazole for size-exclusion).

4.6.4 MurA kinetic Assays. Protocol was done as previously described (elife paper). In short, purified His-SUMO-CwlM$_{Mtb}$ strains (WT and mutants) were either left unphosphorylated or were phosphorylated through a kinase reaction (1:10 His-MPB-PknB to His-SUMO-CwlM, 1mM MnCl2, 0.5mM ATP). Kinase reactions were performed at room temperature in 30uL reactions in kinase buffer; 50 mM Tris pH 7.5, 150 mM NaCl, 1 mM DTT. For unphosphorylated His-SUMO-CwlM, setup was the same but ATP was not added. For kinetic assay, equimolar amounts of His-MurA was added to phosphorylated and non-phosphorylated samples of His-SUMO-CwlM, followed by the addition of substrates; 20mM Phospho-Enol-Pyruvate, 100mM UDP-GlcNac. Samples were then filled to a total volume of 90uL with reaction buffer (50 mM Tris pH 8.0, 2 mM KCl, 2 mM DTT) and incubated at 37C for 30 minutes. After incubation, reaction was stopped

by the addition of 90uL of 0.4M KOH. Samples were then spun/filtered using a microcon filter for 30 minutes, flowthrough for each sample was collected and analyzed through High-Performance Liquid Chromatography (HPLC; Agilent).

4.6.5 Co-Immunopresipitation assay. His-SUMO-CwlM$_{Mtb}$ was first subjected to protease reaction with His-Ulp1 for 30 minutes at room temperature to cleave the His-SUMO tag. CwlM$_{Mtb}$ was then split into two samples, one that would be phosphorylated through a kinase reaction with His-MBP-PknB[5], and a second that would be kept unphosphorylated. His-MurA$_{Mtb}$-strep was then expressed and purified similarly as His-MurA$_{Mtb}$. Pure His-MurA$_{Mtb}$-strep was then immobilized in two microtubes containing magnetic strep beads and washed with PBS buffer. Equimolar CwlM$_{Mtb}$ phosphorylated in PBS was added to one tube containing His-MurA$_{Mtb}$-strep and beads, while equimolar unphosphorylated CwlM$_{Mtb}$ was added to the second tube. Tubes were incubated at room temp for 3 minutes with some "flicking" to avoid settling of beads. Samples were placed in a magnetic rack and supernatant was collected and labeled as flow-through. Tubes were then taken off magnetic rack and resuspended with PBS. Incubation and removal of supernatant were repeated similarly two more times, these samples were labeled as wash 1 and 2. After the second wash, beads were resuspended with 1x Laemmli buffer and cooked for 10 minutes. Tubes were then place on magnetic rack and supernatant collected. These samples were labeled as elution. Flowthrough, washes, and elution were then ran on SDS protein and gel and analyzed with silver stain.

4.6.6 CwlM allele survival. First, *cwlM*$_{Msmeg}$ wild-type and mutant alleles were cloned into a kanamycin-marked L5 integrating vector. These were then transformed into *Msmeg* strains with the native *cwlM* and *murA* knocked out, with nourseothricin-marked wild-type *cwlM* at the L5 integrating site, and either wild-type *murA* (CB737) or suppressor *murA* (CB762) at the tweetie integrating site. Proper swapping and allele survival was scored by the loss of nourseothricin resistance and gain of kanamycin resistance when grown in LB plates. The allele survival was assessed for 150-200 colonies for each *cwlM* allele.

4.6.7 Growth curves of cwlM alleles. Biological triplicate cultures were grown for each *cwlM* allele in both *murA* backgrounds (CB737 & CB762) until log-phase. Growth curves were done on a non-tissue culture treated 96-well plate in 200 uL of 7H9 with a starting OD of 0.1 for each culture. The OD_{600} of each culture was measured every 30 min in a Bioscreen growth curve machine (Growth Curves USA, Piscataway, NJ). Data and doubling time were analyzed using GraphPad Prism software. Doubling time was calculated with a non-linear curve fit method using an exponential growth equation with the least squares fit. p-values were calculated using two-tailed-unpaired t-test.

4.6.8 Cell staining and Microscopy. Triplicate cultures were grown into log-phase in HdB minimal medium. After normalizing to OD 0.3, 1mL of each replicate culture was stained with 1 uL/mL 10 mM HADA (R&D systems) for 15 minutes with rolling incubation at 37C. Post incubation samples were pelleted and resuspended once in 100-200 uL of HdB medium. Cells were then analyzed with a Nikon Ti-2 widefield microscope. A 350/50 nm excitation filter, 460/50 nm emission filter, and a 400 nm dichroic mirror was used to detect HADA signal. The image analysis for each sample was done using the MicrobeJ plugin through the ImageJ (FIJI)

computer software. The mean intensity of about 300 cells per sample was then analyzed using GraphPad prism software.

Chapter 5 – Dissertation Conclusions

As a lab assistant and graduate student in the Boutte lab, I ventured into the intricate world of mycobacteria to learn more about the different mechanisms that allow them to survive during stress. I used *Mycobacterium abscessus (Mab)*, an emerging pathogen notorious for its antibiotic resistance, to uncover crucial insights into its stringent response and biofilm formation. I used a tractable non-pathogenic species, *Mycobacterium smegmatis*, to study the regulatory dynamics between CwlM and MurA in peptidoglycan biosynthesis. Our investigations have unearthed unexpected findings, challenged previous assumptions, and are paving the way for novel therapeutic strategies against challenging pathogens like *Mycobacterium tuberculosis* and *Mab*.

5.1 The stringent response in *Mycobacterium abscessus*

This study elucidated the functional role of the stringent factor Rel in *Mycobacterium abscessus* (*Mab*), as previously mentioned, a pathogen known for its antibiotic resistance. Before our work, no prior studies had analyzed this specific stress response in *Mab*. Unlike in other bacteria, where Rel is the major (p)ppGpp synthase, I found that Rel_{Mab} is not the major synthase of the stress alarmone in *Mab*. Rel_{Mab} also does not promote antibiotic tolerance or survival under clinically relevant stress conditions despite its ability to downregulate metabolic genes. Our findings suggest the existence of another critical but unannotated (p)ppGpp synthetase in *Mab* and highlight the need for further exploration in this area.

Future directions should prioritize identifying and characterizing the additional (p)ppGpp synthetase(s) in *Mab*. Understanding the complete repertoire of enzymes involved in (p)ppGpp synthesis will provide crucial insights into this pathogen's regulatory mechanisms governing antibiotic tolerance and other stress responses. Moreover, our study underscores the limitations

of targeting Rel_{Mab} to sensitize *Mab* infections to antibiotic treatment, emphasizing the importance of alternative approaches in combating this challenging pathogen. Nevertheless, by unraveling the complexity of the stringent response and antibiotic resistance mechanisms in *Mab*, I can develop more effective therapeutic strategies against infections caused by this clinically problematic pathogen.

5.2 The effects of nutrient availability on Mab biofilm formation and antibiotic tolerance

Bacterial biofilms offer physical protection from the environment, including antibiotics, and promote the formation of heterogeneous populations of phenotypically and metabolically different bacteria. In this study, I revealed differences in *Mab* biofilms when grown in media that mimic nutrient conditions found within the lungs of Cystic Fibrosis (CF) patients compared to standard laboratory media. Specifically, I observed distinct surface glycolipid expression patterns, altered biofilm morphology, and increased antibiotic tolerance in *Mab* cultured in Artificial Cystic Fibrosis Sputum (ACFS) media. These findings highlight the importance of environmental factors in shaping *Mab* physiology and suggest that nutrient conditions encountered in the host environment contribute to increased virulence and antibiotic tolerance.

Furthermore, our results emphasize the need to continue researching into the genetics of *Mab* biofilms, specially withing the context of conditions that mimic infection. By clarifying the chemical and genetic basis of biofilm formation and physiological responses in *Mab*, I can better understand the mechanisms underlying treatment recalcitrance and develop improved therapeutic strategies. Future directions may involve exploring molecular pathways to disrupt *Mab* biofilms or prevent their establishment. A comprehensive understanding of *Mab* biofilm physiology in the

context of CF lung infections is crucial for advancing therapeutic approaches and improving patient outcomes.

5.3 CwlM's regulatory interaction with MurA, the first enzyme in peptidoglycan precursor synthesis

This study delved into the intricate interaction between CwlM and MurA, two key players involved in peptidoglycan biosynthesis in mycobacteria. Through computational modeling, biochemical assays, and genetic manipulations, I uncovered new aspects of their interaction and its implications for bacterial physiology. Our computational predictions pinpointed a charged interaction interface between CwlM and MurA. Biochemical assays confirmed the physical interaction between these proteins in vitro, highlighting the functional significance of their association. Importantly, mutations in the predicted interaction site on CwlM led to impairments in MurA activation, emphasizing the essential role of this interface in facilitating enzymatic activity.

Furthermore, our findings suggest that while phosphorylation of CwlM is essential for its interaction with MurA, it alone is insufficient to fully rescue MurA activation, indicating the involvement of additional regulatory mechanisms. I propose a model where phosphorylated CwlM stabilizes MurA in the optimal conformation through the predicted interaction site, thereby promoting and stabilizing its enzymatic activity. Moreover, our study sheds light on the dynamic nature of the CwlM-MurA interaction, demonstrating its transient or weak nature under *in vitro* conditions. This has important implications for understanding the dynamics of peptidoglycan biosynthesis *in vivo* and underscores the complexity of regulatory networks governing bacterial cell wall synthesis. Through genetic approaches, I observed that mutations

affecting MurA activation result in defects in peptidoglycan metabolism, reminding us of the functional relevance of the CwlM-MurA interaction in bacterial cell wall synthesis.

Further elucidation of the regulatory networks governing the CwlM-MurA interaction and its impact on cell wall biosynthesis may pave the way for developing innovative antimicrobial strategies targeting essential bacterial pathways. Future studies should aim to unravel additional factors and modifications involved in modulating the CwlM-MurA interaction and explore its role in the context of mycobacterial pathogenesis. For example, previous data had shown post-translational lysine acetylation on specific lysine residues on CwlM, but the role of this modification on peptidoglycan regulation needs to be further studie. Additionally, investigating the therapeutic potential of targeting this interaction to develop novel antimicrobial agents holds promise in combating drug-resistant mycobacterial infections.

References

1. Tuberculosis. https://www.who.int/health-topics/tuberculosis.

2. Does leprosy still exist? *Leprosy Mission International* https://www.leprosymission.org/what-is-leprosy/does-leprosy-still-exist/?gad_source=1&gclid=CjwKCAiAi6uvBhADEiwAWiyRdsZ-CEE0ui7n9MDK7oN2ELT3n6VhSOowOkPGLC3djxDRHaWATM4qsRoCHbsQAvD_BwE.

3. Lee, M.-R. *et al. Mycobacterium abscessus* Complex Infections in Humans. *Emerg. Infect. Dis.* **21**, (2015).

4. NTM: Treatment. *National Jewish Health* https://www.nationaljewish.org/conditions/ntm-nontuberculous-mycobacteria/ntm-nontuberculous-mycobacteria-overview/treatment.

5. Jang, J. G. & Chung, J. H. Diagnosis and treatment of multidrug-resistant tuberculosis. *Yeungnam Univ J Med* **37**, 277–285 (2020).

6. Centers for Disease Control and Prevention. Historical Perspectives Centennial: Koch's Discovery of the Tubercle Bacillus. *MMWR* https://www.cdc.gov/mmwr/preview/mmwrhtml/00000222.htm.

7. Nahid, P. *et al.* Executive Summary: Official American Thoracic Society/Centers for Disease Control and Prevention/Infectious Diseases Society of America Clinical Practice Guidelines: Treatment of Drug-Susceptible Tuberculosis. *Clinical Infectious Diseases* **63**, 853–867 (2016).

8. Padda, I. S. & Muralidhara Reddy, K. Antitubercular Medications. in *StatPearls* (StatPearls Publishing, Treasure Island (FL), 2024).

9. CDCTB. Tuberculosis (TB) - Treatment Regimens for Latent TB Infection. *Centers for Disease Control and Prevention* https://www.cdc.gov/tb/topic/treatment/default.htm (2023).

10. Urdahl, K. B., Shafiani, S. & Ernst, J. D. Initiation and regulation of T-cell responses in tuberculosis. *Mucosal Immunol* **4**, 288–293 (2011).

11. Pai, M. *et al.* Tuberculosis. *Nat Rev Dis Primers* **2**, 16076 (2016).

12. Pagán, A. J. & Ramakrishnan, L. The Formation and Function of Granulomas. *Annu. Rev. Immunol.* **36**, 639–665 (2018).

13. Miranda, M. S., Breiman, A., Allain, S., Deknuydt, F. & Altare, F. The Tuberculous Granuloma: An Unsuccessful Host Defence Mechanism Providing a Safety Shelter for the Bacteria? *Clinical and Developmental Immunology* 15.

14. Martin, C. J., Carey, A. F. & Fortune, S. M. A bug's life in the granuloma. *Semin Immunopathol* **38**, 213–220 (2016).

15. Bold, T. D. & Ernst, J. D. Who Benefits from Granulomas, Mycobacteria or Host? *Cell* **136**, 17–19 (2009).

16. Rubin, E. J. The Granuloma in Tuberculosis — Friend or Foe? *N Engl J Med* **360**, 2471–2473 (2009).

17. Pagán, A. J. & Ramakrishnan, L. Immunity and Immunopathology in the Tuberculous Granuloma. *Cold Spring Harb Perspect Med* **5**, a018499 (2015).

18. Abdelaal, H. F. M., Chan, E. D., Young, L., Baldwin, S. L. & Coler, R. N. Mycobacterium abscessus: It's Complex. *Microorganisms* **10**, 1454 (2022).

19. Ferrell, K. C., Johansen, M. D., Triccas, J. A. & Counoupas, C. Virulence Mechanisms of Mycobacterium abscessus: Current Knowledge and Implications for Vaccine Design. *Front. Microbiol.* **13**, 842017 (2022).

20. Falkinham, Iii, J. O. Surrounded by mycobacteria: nontuberculous mycobacteria in the human environment. *Journal of Applied Microbiology* **107**, 356–367 (2009).

21. Nash, K. A., Brown-Elliott, B. A. & Wallace, R. J. A Novel Gene, erm(41), Confers Inducible Macrolide Resistance to Clinical Isolates of Mycobacterium abscessus but Is Absent from Mycobacterium chelonae. *AAC* **53**, 1367–1376 (2009).

22. Nessar, R., Cambau, E., Reyrat, J. M., Murray, A. & Gicquel, B. Mycobacterium abscessus: a new antibiotic nightmare. *Journal of Antimicrobial Chemotherapy* **67**, 810–818 (2012).

23. Boutte, C. C. & Crosson, S. Bacterial lifestyle shapes stringent response activation. *Trends in Microbiology* **21**, 174–180 (2013).

24. Primm, T. P. *et al.* The Stringent Response of Mycobacterium tuberculosis Is Required for Long-Term Survival. *Journal of Bacteriology* **182**, 4889–4898 (2000).

25. Dutta, N. K. *et al.* Inhibiting the stringent response blocks Mycobacterium tuberculosis entry into quiescence and reduces persistence. *Science Advances* **5**, eaav2104 (2019).

26. Cashel, M. & Gallant, J. Two Compounds implicated in the Function of the RC Gene of Escherichia coli. *Nature* **221**, 838 (1969).

27. Irving, S. E., Choudhury, N. R. & Corrigan, R. M. The stringent response and physiological roles of (pp)pGpp in bacteria. *Nat Rev Microbiol* **19**, 256–271 (2021).

28. Balzer, G. J. & McLean, R. J. C. The stringent response genes relA and spoT are important for Escherichia coli biofilms under slow-growth conditions. **48**, 6 (2002).

29. Steinchen, W. & Bange, G. The magic dance of the alarmones (p)ppGpp: The structural biology of the alarmones (p)ppGpp. *Molecular Microbiology* **101**, 531–544 (2016).

30. Hobbs, J. K. & Boraston, A. B. (p)ppGpp and the Stringent Response: An Emerging Threat to Antibiotic Therapy. *ACS Infect. Dis.* **5**, 1505–1517 (2019).

31. Tripathi, P., Singh, L. K., Kumari, S., Hakiem, O. R. & Batra, J. K. ClpB is an essential stress regulator of Mycobacterium tuberculosis and endows survival advantage to dormant bacilli. *International Journal of Medical Microbiology* **310**, 151402 (2020).

32. Namouchi, A. *et al.* The Mycobacterium tuberculosis transcriptional landscape under genotoxic stress. *BMC Genomics* **17**, 791 (2016).

33. Rominski, A., Roditscheff, A., Selchow, P., Böttger, E. C. & Sander, P. Intrinsic rifamycin resistance of Mycobacterium abscessus is mediated by ADP-ribosyltransferase MAB_0591. *J Antimicrob Chemother* **72**, 376–384 (2017).

34. Dubois, V. *et al.* Mycobacterium abscessus virulence traits unraveled by transcriptomic profiling in amoeba and macrophages. *PLoS Pathog* **15**, e1008069 (2019).

35. Hurst-Hess, K., Rudra, P. & Ghosh, P. Mycobacterium abscessus WhiB7 Regulates a Species-Specific Repertoire of Genes To Confer Extreme Antibiotic Resistance. *Antimicrobial Agents and Chemotherapy* **61**, (2017).

36. Petchiappan, A., Naik, S. Y. & Chatterji, D. RelZ-mediated stress response in *Mycobacterium smegmatis* : pGpp synthesis and its regulation. *J Bacteriol* JB.00444-19, jb;JB.00444-19v1 (2019) doi:10.1128/JB.00444-19.

37. Dokic, A. *et al.* Mycobacterium abscessus biofilms produce an extracellular matrix and have a distinct mycolic acid profile. *The Cell Surface* **7**, 100051 (2021).

38. Aung, T. T. *et al.* Discovery of novel antimycobacterial drug therapy in biofilm of pathogenic nontuberculous mycobacterial keratitis. *The Ocular Surface* **15**, 770–783 (2017).

39. Faria, S., Joao, I. & Jordao, L. General Overview on Nontuberculous Mycobacteria, Biofilms, and Human Infection. *Journal of Pathogens* **2015**, 1–10 (2015).

40. Roux, A.-L. *et al.* The distinct fate of smooth and rough *Mycobacterium abscessus* variants inside macrophages. *Open Biol.* **6**, 160185 (2016).

41. Howard, S. T. Spontaneous reversion of Mycobacterium abscessus from a smooth to a rough morphotype is associated with reduced expression of glycopeptidolipid and reacquisition of an invasive phenotype. *Microbiology* **152**, 1581–1590 (2006).

42. Gutiérrez, A. V., Viljoen, A., Ghigo, E., Herrmann, J.-L. & Kremer, L. Glycopeptidolipids, a Double-Edged Sword of the Mycobacterium abscessus Complex. *Frontiers in Microbiology* **9**, (2018).

43. Pawlik, A. *et al.* Identification and characterization of the genetic changes responsible for the characteristic smooth-to-rough morphotype alterations of clinically persistent *Mycobacterium abscessus*: Genetic traits of rough mutants of *Mycobacterium abscessus*. *Molecular Microbiology* **90**, 612–629 (2013).

44. Clary, G. *et al. Mycobacterium abscessus* Smooth and Rough Morphotypes Form Antimicrobial-Tolerant Biofilm Phenotypes but Are Killed by Acetic Acid. *Antimicrobial Agents and Chemotherapy* **62**, (2018).

45. Jonsson, B. E. *et al.* Molecular Epidemiology of Mycobacterium abscessus, with Focus on Cystic Fibrosis. *Journal of Clinical Microbiology* **45**, 1497–1504 (2007).

46. Zambrano, M. M. & Kolter, R. Mycobacterial Biofilms: A Greasy Way to Hold It Together. *Cell* **123**, 762–764 (2005).

47. Dulberger, C. L., Rubin, E. J. & Boutte, C. C. The mycobacterial cell envelope — a moving target. *Nat Rev Microbiol* (2019) doi:10.1038/s41579-019-0273-7.

48. Forrellad, M. A. *et al.* Virulence factors of the *Mycobacterium tuberculosis* complex. *Virulence* **4**, 3–66 (2013).

49. Gram Stain: MedlinePlus Medical Test. https://medlineplus.gov/lab-tests/gram-stain/.

50. Acid-Fast - an overview | ScienceDirect Topics. https://www.sciencedirect.com/topics/medicine-and-dentistry/acid-fast.

51. Vollmer, W. & Bertsche, U. Murein (peptidoglycan) structure, architecture and biosynthesis in Escherichia coli. *Biochimica et Biophysica Acta (BBA) - Biomembranes* **1778**, 1714–1734 (2008).

52. Maitra, A. *et al.* Cell wall peptidoglycan in Mycobacterium tuberculosis: An Achilles' heel for the TB-causing pathogen. *FEMS Microbiology Reviews* **43**, 548–575 (2019).

53. Kurosu, M., Mahapatra, S., Narayanasamy, P. & Crick, D. C. Chemoenzymatic synthesis of Park's nucleotide: toward the development of high-throughput screening for MraY inhibitors. *Tetrahedron Letters* **48**, 799–803 (2007).

54. Kuk, A. C. Y., Hao, A., Guan, Z. & Lee, S.-Y. Visualizing conformation transitions of the Lipid II flippase MurJ. *Nat Commun* **10**, 1736 (2019).

55. Deng, J. *et al.* Mycobacterium Tuberculosis Proteome Microarray for Global Studies of Protein Function and Immunogenicity. *Cell Reports* **9**, 2317–2329 (2014).

56. Wang, C. *et al.* Effects of CwlM on autolysis and biofilm formation in Mycobacterium tuberculosis and Mycobacterium smegmatis. *International Journal of Medical Microbiology* **309**, 73–83 (2019).

57. Deng, L. L. *et al.* Identification of a novel peptidoglycan hydrolase CwlM in Mycobacterium tuberculosis. *Biochimica et Biophysica Acta (BBA) - Proteins and Proteomics* **1747**, 57–66 (2005).

58. Boutte, C. C. *et al.* A cytoplasmic peptidoglycan amidase homologue controls mycobacterial cell wall synthesis. *eLife* **5**, (2016).

59. Turapov, O. *et al.* Two Faces of CwlM, an Essential PknB Substrate, in Mycobacterium tuberculosis. *Cell Rep* **25**, 57-67.e5 (2018).

60. Dahl, J. L. *et al.* The role of RelMtb-mediated adaptation to stationary phase in long-term persistence of Mycobacterium tuberculosis in mice. *Proceedings of the National Academy of Sciences* **100**, 10026–10031 (2003).

61. Traxler, M. F. *et al.* The global, ppGpp-mediated stringent response to amino acid starvation in Escherichia coli. *Molecular Microbiology* **68**, 1128–1148 (2008).

62. Boutte, C. C. & Crosson, S. The complex logic of stringent response regulation in Caulobacter crescentus: starvation signalling in an oligotrophic environment. *Molecular Microbiology* **80**, 695–714 (2011).

63. Hauryliuk, V., Atkinson, G. C., Murakami, K. S., Tenson, T. & Gerdes, K. Recent functional insights into the role of (p)ppGpp in bacterial physiology. *Nat Rev Microbiol* **13**, 298–309 (2015).

64. Harms, A., Fino, C., Sørensen, M. A., Semsey, S. & Gerdes, K. Prophages and Growth Dynamics Confound Experimental Results with Antibiotic-Tolerant Persister Cells. *mBio* **8**, (2017).

65. Johansen, M. D., Herrmann, J.-L. & Kremer, L. Non-tuberculous mycobacteria and the rise of Mycobacterium abscessus. *Nat Rev Microbiol* (2020) doi:10.1038/s41579-020-0331-1.

66. Hunt-Serracin, A. C., Parks, B. J., Boll, J. & Boutte, C. Biofilm-associated Mycobacterium abscessus cells have altered antibiotic tolerance and surface glycolipids in Artificial Cystic Fibrosis Sputum Media. *Antimicrobial Agents and Chemotherapy* AAC.02488-18 (2019) doi:10.1128/AAC.02488-18.

67. Wexselblatt, E. *et al.* Relacin, a Novel Antibacterial Agent Targeting the Stringent Response. *PLOS Pathogens* **8**, e1002925 (2012).

68. Dutta, N. K. *et al.* Inhibiting the stringent response blocks *Mycobacterium tuberculosis* entry into quiescence and reduces persistence. *Science Advances* **5**, eaav2104 (2019).

69. Pacios, O. *et al.* (p)ppGpp and Its Role in Bacterial Persistence: New Challenges. *Antimicrob Agents Chemother* **64**, e01283-20, /aac/64/10/AAC.01283-20.atom (2020).

70. Barker, M. M., Gaal, T., Josaitis, C. A. & Gourse, R. L. Mechanism of regulation of transcription initiation by ppGpp. I. Effects of ppGpp on transcription initiation in vivo and in vitro1 1Edited by R. Ebright. *Journal of Molecular Biology* **305**, 673–688 (2001).

71. Barker, M. M., Gaal, T. & Gourse, R. L. Mechanism of regulation of transcription initiation by ppGpp. II. Models for positive control based on properties of RNAP mutants and competition for RNAP11Edited by R. Ebright. *Journal of Molecular Biology* **305**, 689–702 (2001).

72. Krásný, L. & Gourse, R. L. An alternative strategy for bacterial ribosome synthesis: Bacillus subtilis rRNA transcription regulation. *EMBO J* **23**, 4473–4483 (2004).

73. Krásný, L., Tišerová, H., Jonák, J., Rejman, D. & Šanderová, H. The identity of the transcription +1 position is crucial for changes in gene expression in response to amino acid starvation in Bacillus subtilis. *Molecular Microbiology* **69**, 42–54 (2008).

74. Maciąg, M., Kochanowska, M., Łyżeń, R., Węgrzyn, G. & Szalewska-Pałasz, A. ppGpp inhibits the activity of Escherichia coli DnaG primase. *Plasmid* **63**, 61–67 (2010).

75. Kraemer, J. A., Sanderlin, A. G. & Laub, M. T. The Stringent Response Inhibits DNA Replication Initiation in *E. coli* by Modulating Supercoiling of *oriC*. *mBio* **10**, e01330-19, /mbio/10/4/mBio.01330-19.atom (2019).

76. Kriel, A. *et al.* Direct Regulation of GTP Homeostasis by (p)ppGpp: A Critical Component of Viability and Stress Resistance. *Molecular Cell* **48**, 231–241 (2012).

77. Wang, B. *et al.* Affinity-based capture and identification of protein effectors of the growth regulator ppGpp. *Nature Chemical Biology* **15**, 141–150 (2019).

78. Wang, B., Grant, R. A. & Laub, M. T. ppGpp Coordinates Nucleotide and Amino-Acid Synthesis in E. coli During Starvation. *Molecular Cell* S1097276520305487 (2020) doi:10.1016/j.molcel.2020.08.005.

79. Fan, H., Hahm, J., Diggs, S., Perry, J. J. P. & Blaha, G. Structural and Functional Analysis of BipA, a Regulator of Virulence in Enteropathogenic *Escherichia coli*. *J. Biol. Chem.* **290**, 20856–20864 (2015).

80. Corrigan, R. M., Bellows, L. E., Wood, A. & Gründling, A. ppGpp negatively impacts ribosome assembly affecting growth and antimicrobial tolerance in Gram-positive bacteria. *Proc Natl Acad Sci USA* **113**, E1710–E1719 (2016).

81. Rojas, A.-M., Ehrenberg, M., Andersson, S. G. E. & Kurland, C. G. ppGpp inhibition of elongation factors Tu, G and Ts during polypeptide synthesis. *Mol Gen Genet* **197**, 36–45 (1984).

82. Milon, P. *et al.* The nucleotide-binding site of bacterial translation initiation factor 2 (IF2) as a metabolic sensor. *Proceedings of the National Academy of Sciences* **103**, 13962–13967 (2006).

83. Mitkevich, V. A. *et al.* Thermodynamic Characterization of ppGpp Binding to EF-G or IF2 and of Initiator tRNA Binding to Free IF2 in the Presence of GDP, GTP, or ppGpp. *Journal of Molecular Biology* **402**, 838–846 (2010).

84. Atkinson, G. C., Tenson, T. & Hauryliuk, V. The RelA/SpoT Homolog (RSH) Superfamily: Distribution and Functional Evolution of ppGpp Synthetases and Hydrolases across the Tree of Life. *PLoS ONE* **6**, e23479 (2011).

85. Haseltine, W. A. & Block, R. Synthesis of Guanosine Tetra- and Pentaphosphate Requires the Presence of a Codon-Specific, Uncharged Transfer Ribonucleic Acid in the Acceptor Site of Ribosomes. *Proc Natl Acad Sci U S A* **70**, 1564–1568 (1973).

86. Ronneau, S. & Hallez, R. Make and break the alarmone: regulation of (p)ppGpp synthetase/hydrolase enzymes in bacteria. *FEMS Microbiology Reviews* **43**, 389–400 (2019).

87. Battesti, A. & Bouveret, E. Acyl carrier protein/SpoT interaction, the switch linking SpoT-dependent stress response to fatty acid metabolism. *Molecular Microbiology* **62**, 1048–1063 (2006).

88. Brown, D. R., Barton, G., Pan, Z., Buck, M. & Wigneshweraraj, S. Nitrogen stress response and stringent response are coupled in Escherichia coli. *Nat Commun* **5**, 4115 (2014).

89. Ronneau, S., Petit, K., De Bolle, X. & Hallez, R. Phosphotransferase-dependent accumulation of (p)ppGpp in response to glutamine deprivation in Caulobacter crescentus. *Nat Commun* **7**, 11423 (2016).

90. Germain, E. *et al.* YtfK activates the stringent response by triggering the alarmone synthetase SpoT in Escherichia coli. *Nat Commun* **10**, 5763 (2019).

91. Nanamiya, H. *et al.* Identification and functional analysis of novel (p)ppGpp synthetase genes in Bacillus subtilis: Novel (p)ppGpp synthetase genes in B. subtilis. *Molecular Microbiology* **67**, 291–304 (2007).

92. Ruwe, M., Kalinowski, J. & Persicke, M. Identification and Functional Characterization of Small Alarmone Synthetases in Corynebacterium glutamicum. *Front Microbiol* **8**, 1601 (2017).

93. Ruwe, M., Rückert, C., Kalinowski, J. & Persicke, M. Functional Characterization of a Small Alarmone Hydrolase in Corynebacterium glutamicum. *Front. Microbiol.* **9**, 916 (2018).

94. Yang, N. *et al.* The Ps and Qs of alarmone synthesis in Staphylococcus aureus. *PLoS ONE* **14**, e0213630 (2019).

95. Jimmy, S. *et al.* A widespread toxin−antitoxin system exploiting growth control via alarmone signaling. *Proc Natl Acad Sci USA* **117**, 10500–10510 (2020).

96. Jones, G. H. Purification and properties of ATP:GTP 3'-pyrophosphotransferase (guanosine pentaphosphate synthetase) from Streptomyces antibioticus. *J Bacteriol* **176**, 1475–1481 (1994).

97. Jones, G. H. Activation of ATP:GTP 3'-pyrophosphotransferase (guanosine pentaphosphate synthetase) in Streptomyces antibioticus. *J Bacteriol* **176**, 1482–1487 (1994).

98. Jones, G. H. & Bibb, M. J. Guanosine pentaphosphate synthetase from Streptomyces antibioticus is also a polynucleotide phosphorylase. *Journal of bacteriology* **178**, 4281–4288 (1996).

99. Jones, G. H. Novel Aspects of Polynucleotide Phosphorylase Function in Streptomyces. *Antibiotics (Basel)* **7**, 25 (2018).

100. Schofield, W. B., Zimmermann-Kogadeeva, M., Zimmermann, M., Barry, N. A. & Goodman, A. L. The Stringent Response Determines the Ability of a Commensal Bacterium to Survive Starvation and to Persist in the Gut. *Cell Host & Microbe* **24**, 120-132.e6 (2018).

101. Eymann, C., Homuth, G., Scharf, C. & Hecker, M. Bacillus subtilis functional genomics: global characterization of the stringent response by proteome and transcriptome analysis. *JB* **184**, 2500–2520 (2002).

102. Potrykus, K., Murphy, H., Philippe, N. & Cashel, M. ppGpp is the major source of growth rate control in E. coli. *Environmental Microbiology* **13**, 563–575 (2011).

103. Weiss, L. A. & Stallings, C. L. Essential Roles for Mycobacterium tuberculosis Rel beyond the Production of (p)ppGpp. *Journal of Bacteriology* **195**, 5629–5638 (2013).

104. Pulschen, A. A. *et al.* The stringent response plays a key role in Bacillus subtilis survival of fatty acid starvation. *Molecular Microbiology* **103**, 698–712 (2017).

105. Murch, A. L., Skipp, P. J., Roach, P. L. & Oyston, P. C. F. Whole genome transcriptomics reveals global effects including up-regulation of Francisella pathogenicity island gene expression during active stringent response in the highly virulent Francisella tularensis subsp. tularensis SCHU S4. *Microbiology* **163**, 1664–1679 (2017).

106. Schäfer, H. *et al.* The alarmones (p)ppGpp are part of the heat shock response of Bacillus subtilis. *PLoS Genet* **16**, e1008275 (2020).

107. Stallings, C. L. *et al.* CarD Is an Essential Regulator of rRNA Transcription Required for Mycobacterium tuberculosis Persistence. *Cell* **138**, 146–159 (2009).

108. Klinkenberg, L. G., Lee, J., Bishai, W. R. & Karakousis, P. C. The Stringent Response Is Required for Full Virulence of *Mycobacterium tuberculosis* in Guinea Pigs. *J INFECT DIS* **202**, 1397–1404 (2010).

109. Prusa, J., Zhu, D. X. & Stallings, C. L. The stringent response and Mycobacterium tuberculosis pathogenesis. *Pathogens and Disease; Oxford* **76**, (2018).

110. Njire, M. *et al.* Pyrazinoic Acid Inhibits a Bifunctional Enzyme in Mycobacterium tuberculosis. *Antimicrob Agents Chemother* **61**, e00070-17, e00070-17 (2017).

111. Dahl, J. L. *et al.* The relA Homolog of Mycobacterium smegmatis Affects Cell Appearance, Viability, and Gene Expression. *Journal of Bacteriology* **187**, 2439–2447 (2005).

112. Jain, V., Saleem-Batcha, R., China, A. & Chatterji, D. Molecular dissection of the mycobacterial stringent response protein Rel. *Protein Science* **15**, 1449–1464 (2006).

113. Murdeshwar, M. S. & Chatterji, D. MS_RHII-RSD, a Dual-Function RNase HII-(p)ppGpp Synthetase from Mycobacterium smegmatis. *Journal of Bacteriology* **194**, 4003–4014 (2012).

114. Ojha, A. K., Mukherjee, T. K. & Chatterji, D. High Intracellular Level of Guanosine Tetraphosphate in Mycobacterium smegmatis Changes the Morphology of the Bacterium. *Infect Immun* **68**, 4084–4091 (2000).

115. Gupta, K. R., Kasetty, S. & Chatterji, D. Novel Functions of (p)ppGpp and Cyclic di-GMP in Mycobacterial Physiology Revealed by Phenotype Microarray Analysis of Wild-Type and Isogenic Strains of Mycobacterium smegmatis. *Appl. Environ. Microbiol.* **81**, 2571–2578 (2015).

116. Sugisaki, K. *et al.* Role of (p)ppGpp in biofilm formation and expression of filamentous structures in Bordetella pertussis. *Microbiology* **159**, 1379–1389 (2013).

117. Oh, Y. T., Lee, K.-M., Bari, W., Raskin, D. M. & Yoon, S. S. (p)ppGpp, a Small Nucleotide Regulator, Directs the Metabolic Fate of Glucose in *Vibrio cholerae*. *J. Biol. Chem.* **290**, 13178–13190 (2015).

118. Kim, J.-S. *et al.* DksA–DnaJ redox interactions provide a signal for the activation of bacterial RNA polymerase. *Proceedings of the National Academy of Sciences* **115**, E11780–E11789 (2018).

119. Gaca, A. O. *et al.* Basal Levels of (p)ppGpp in Enterococcus faecalis: the Magic beyond the Stringent Response. *mBio* **4**, e00646-13 (2013).

120. Novosad, S. A., Beekmann, S. E., Polgreen, P. M., Mackey, K. & Winthrop, K. L. Treatment of Mycobacterium abscessus Infection. *Emerg Infect Dis* **22**, 511–514 (2016).

121. Cabral, D. J., Wurster, J. I. & Belenky, P. Antibiotic Persistence as a Metabolic Adaptation: Stress, Metabolism, the Host, and New Directions. *Pharmaceuticals (Basel)* **11**, (2018).

122. Fenn, K., Wong, C. T. & Darbari, V. C. Mycobacterium tuberculosis Uses Mce Proteins to Interfere With Host Cell Signaling. *Front. Mol. Biosci.* **6**, 149 (2020).

123. Brockmann-Gretza, O. & Kalinowski, J. Global gene expression during stringent response in Corynebacterium glutamicum in presence and absence of the rel gene encoding (p)ppGpp synthase. *BMC Genomics* **7**, 230 (2006).

124. Traxler, M. F. *et al.* The global, ppGpp-mediated stringent response to amino acid starvation in Escherichia coli. *Molecular Microbiology* **68**, 1128–1148 (2008).

125. Vercruysse, M. *et al.* Stress response regulators identified through genome-wide transcriptome analysis of the (p)ppGpp-dependent response in Rhizobium etli. *Genome Biol* **12**, R17 (2011).

126. Yang, H., Yu, M., Lee, J. H., Chatnaparat, T. & Zhao, Y. The stringent response regulator (p) ppGpp mediates virulence gene expression and survival in Erwinia amylovora. *BMC Genomics* **21**, 261 (2020).

127. Traxler, M. F. *et al.* Discretely calibrated regulatory loops controlled by ppGpp partition gene induction across the 'feast to famine' gradient in Escherichia coli: Architecture of the stringent response. *Molecular Microbiology* **79**, 830–845 (2011).

128. Ross, W., Vrentas, C. E., Sanchez-Vazquez, P., Gaal, T. & Gourse, R. L. The Magic Spot: A ppGpp Binding Site on E. coli RNA Polymerase Responsible for Regulation of Transcription Initiation. *Molecular Cell* 10.

129. Jayasingam, S., Zin, T. & Ngeow, Y. Antibiotic resistance in Mycobacterium Abscessus and Mycobacterium Fortuitum isolates from Malaysian patients. *Int J Mycobacteriol* **6**, 387 (2017).

130. Luthra, S., Rominski, A. & Sander, P. The Role of Antibiotic-Target-Modifying and Antibiotic-Modifying Enzymes in Mycobacterium abscessus Drug Resistance. *Front Microbiol* **9**, (2018).

131. Bar-On, O. *et al.* Increasing nontuberculous mycobacteria infection in cystic fibrosis. *Journal of Cystic Fibrosis* **14**, 53–62 (2015).

132. Koskiniemi, S., Pränting, M., Gullberg, E., Näsvall, J. & Andersson, D. I. Activation of cryptic aminoglycoside resistance in Salmonella enterica: Activation of cryptic resistance. *Molecular Microbiology* **80**, 1464–1478 (2011).

133. Aedo, S. & Tomasz, A. Role of the Stringent Stress Response in the Antibiotic Resistance Phenotype of Methicillin-Resistant Staphylococcus aureus. *Antimicrob. Agents Chemother.* **60**, 2311–2317 (2016).

134. van Kessel, J. C. & Hatfull, G. F. Recombineering in Mycobacterium tuberculosis. *Nat Methods* **4**, 147–152 (2007).

135. Kieser, K. J. *et al.* Phosphorylation of the Peptidoglycan Synthase PonA1 Governs the Rate of Polar Elongation in Mycobacteria. *PLOS Pathogens* **11**, e1005010 (2015).

136. Hartmans, S., de Bont, J. A. M. & Stackebrandt, E. The Genus Mycobacterium--Nonmedical. in *The Prokaryotes* (eds. Dworkin, M., Falkow, S., Rosenberg, E., Schleifer, K.-H. & Stackebrandt, E.) 889–918 (Springer New York, New York, NY, 2006). doi:10.1007/0-387-30743-5_33.

137. Shell, S. S. *et al.* DNA Methylation Impacts Gene Expression and Ensures Hypoxic Survival of Mycobacterium tuberculosis. *PLoS Pathog* **9**, e1003419 (2013).

138. Livak, K. J. & Schmittgen, T. D. Analysis of Relative Gene Expression Data Using Real-Time Quantitative PCR and the 2−ΔΔCT Method. *Methods* **25**, 402–408 (2001).

139. Brode, S. K., Daley, C. L. & Marras, T. K. The epidemiologic relationship between tuberculosis and non- tuberculous mycobacterial disease: a systematic review. 9.

140. Stout, J. E., Koh, W.-J. & Yew, W. W. Update on pulmonary disease due to non-tuberculous mycobacteria. *International Journal of Infectious Diseases* **45**, 123–134 (2016).

141. Esther, C. R., Esserman, D. A., Gilligan, P., Kerr, A. & Noone, P. G. Chronic Mycobacterium abscessus infection and lung function decline in cystic fibrosis. *Journal of Cystic Fibrosis* **9**, 117–123 (2010).

142. Bryant, J. M. *et al.* Emergence and spread of a human-transmissible multidrug-resistant nontuberculous mycobacterium. *Science* **354**, 751–757 (2016).

143. DaCosta, A. *et al.* Outcomes associated with antibiotic regimens for treatment of Mycobacterium abscessus in cystic fibrosis patients. *Journal of Cystic Fibrosis* **16**, 483–487 (2017).

144. Rominski, A. *et al.* Elucidation of Mycobacterium abscessus aminoglycoside and capreomycin resistance by targeted deletion of three putative resistance genes. *J Antimicrob Chemother* **72**, 2191–2200 (2017).

145. Greendyke, R. & Byrd, T. F. Differential Antibiotic Susceptibility of Mycobacterium abscessus Variants in Biofilms and Macrophages Compared to That of Planktonic Bacteria. *Antimicrobial Agents and Chemotherapy* **52**, 2019–2026 (2008).

146. Qvist, T. *et al.* Chronic pulmonary disease with *Mycobacterium abscessus* complex is a biofilm infection. *European Respiratory Journal* **46**, 1823–1826 (2015).

147. Flemming, H.-C., Neu, T. R. & Wozniak, D. J. The EPS Matrix: The 'House of Biofilm Cells'. *Journal of Bacteriology* **189**, 7945–7947 (2007).

148. Recht, J., Martinez, A., Torello, S. & Kolter, R. Genetic Analysis of Sliding Motility in Mycobacterium smegmatis. *Journal of Bacteriology* **182**, 4348–4351 (2000).

149. Ojha, A. *et al.* GroEL1: A Dedicated Chaperone Involved in Mycolic Acid Biosynthesis during Biofilm Formation in Mycobacteria. *Cell* **123**, 861–873 (2005).

150. Ojha, A. K. *et al.* Growth of *Mycobacterium tuberculosis* biofilms containing free mycolic acids and harbouring drug-tolerant bacteria. *Molecular Microbiology* **69**, 164–174 (2008).

151. Stewart, P. S. Antimicrobial Tolerance in Biofilms. *Microbiology Spectrum* **3**, (2015).

152. Davidson, L. B., Nessar, R., Kempaiah, P., Perkins, D. J. & Byrd, T. F. Mycobacterium abscessus Glycopeptidolipid Prevents Respiratory Epithelial TLR2 Signaling as Measured by HβD2 Gene Expression and IL-8 Release. *PLoS ONE* **6**, e29148 (2011).

153. Hunter, R. L., Olsen, M. R., Jagannath, C. & Actor, J. K. Multiple Roles of Cord Factor in the Pathogenesis of Primary, Secondary, and Cavitary Tuberculosis, Including a Revised Description of the Pathology of Secondary Disease. *Ann Clin Lab Sci* **36**, 371–386 (2006).

154. Byrd, T. F. & Lyons, C. R. Preliminary Characterization of a Mycobacterium abscessus Mutant in Human and Murine Models of Infection. *INFECT. IMMUN.* **67**, 8 (1999).

155. Kreutzfeldt, K. M. *et al.* Molecular Longitudinal Tracking of Mycobacterium abscessus spp. during Chronic Infection of the Human Lung. *PLoS ONE* **8**, e63237 (2013).

156. Park, I. K. *et al.* Clonal Diversification and Changes in Lipid Traits and Colony Morphology in Mycobacterium abscessus Clinical Isolates. *Journal of Clinical Microbiology* **53**, 3438–3447 (2015).

157. Palmer, K. L., Aye, L. M. & Whiteley, M. Nutritional Cues Control *Pseudomonas aeruginosa* Multicellular Behavior in Cystic Fibrosis Sputum. *J Bacteriol* **189**, 8079–8087 (2007).

158. Kuru, E. *et al.* In Situ Probing of Newly Synthesized Peptidoglycan in Live Bacteria with Fluorescent D -Amino Acids. *Angewandte Chemie International Edition* **51**, 12519–12523 (2012).

159. Fishov, I. & Woldringh, C. L. Visualization of membrane domains in *Escherichia coli*. *Molecular Microbiology* **32**, 1166–1172 (1999).

160. Aldridge, B. B. *et al.* Asymmetry and Aging of Mycobacterial Cells Lead to Variable Growth and Antibiotic Susceptibility. *Science* **335**, 100–104 (2012).

161. Burbaud, S. *et al.* Trehalose Polyphleates Are Produced by a Glycolipid Biosynthetic Pathway Conserved across Phylogenetically Distant Mycobacteria. *Cell Chemical Biology* **23**, 278–289 (2016).

162. Wayne, L. G. & Hayes, L. G. An In Vitro Model for Sequential Study of Shiftdown of Mycobacterium tuberculosis through Two Stages of Nonreplicating Persistence. *INFECT. IMMUN.* **64**, 8 (1996).

163. Varma, S., Ojha, A. Kr. & Chatterji, D. Synthesis of an unusual polar glycopeptidolipid in glucose-limited culture of Mycobacterium smegmatis. *Microbiology* **148**, 3039–3048 (2002).

164. Blair, J. M. A., Richmond, G. E., Bailey, A. M., Ivens, A. & Piddock, L. J. V. Choice of Bacterial Growth Medium Alters the Transcriptome and Phenotype of Salmonella enterica Serovar Typhimurium. *PLoS ONE* **8**, e63912 (2013).

165. Kostakioti, M., Hadjifrangiskou, M. & Hultgren, S. J. Bacterial Biofilms: Development, Dispersal, and Therapeutic Strategies in the Dawn of the Postantibiotic Era. *Cold Spring Harbor Perspectives in Medicine* **3**, a010306–a010306 (2013).

166. Landry, R. M., An, D., Hupp, J. T., Singh, P. K. & Parsek, M. R. Mucin-Pseudomonas aeruginosa interactions promote biofilm formation and antibiotic resistance. *Molecular Microbiology* **59**, 142–151 (2006).

167. Jackson, L. M. D., Kroukamp, O. & Wolfaardt, G. M. Effect of carbon on whole-biofilm metabolic response to high doses of streptomycin. *Frontiers in Microbiology* **6**, (2015).

168. Serra, D. O., Richter, A. M., Klauck, G., Mika, F. & Hengge, R. Microanatomy at Cellular Resolution and Spatial Order of Physiological Differentiation in a Bacterial Biofilm. *mBio* **4**, (2013).

169. Besharova, O., Suchanek, V. M., Hartmann, R., Drescher, K. & Sourjik, V. Diversification of Gene Expression during Formation of Static Submerged Biofilms by Escherichia coli. *Frontiers in Microbiology* **7**, (2016).

170. Williamson, K. S. *et al.* Heterogeneity in Pseudomonas aeruginosa Biofilms Includes Expression of Ribosome Hibernation Factors in the Antibiotic-Tolerant Subpopulation and Hypoxia-Induced Stress Response in the Metabolically Active Population. *Journal of Bacteriology* **194**, 2062–2073 (2012).

171. Xie, Z., Siddiqi, N. & Rubin, E. J. Differential Antibiotic Susceptibilities of Starved Mycobacterium tuberculosis Isolates. *Antimicrobial Agents and Chemotherapy* **49**, 4778–4780 (2005).

172. Sriramulu, D. D. Microcolony formation: a novel biofilm model of Pseudomonas aeruginosa for the cystic fibrosis lung. *Journal of Medical Microbiology* **54**, 667–676 (2005).

173. Varma, S., Ojha, A. Kr. & Chatterji, D. Synthesis of an unusual polar glycopeptidolipid in glucose-limited culture of Mycobacterium smegmatis. *Microbiology* **148**, 3039–3048 (2002).

174. Ducret, A., Quardokus, E. M. & Brun, Y. V. MicrobeJ, a tool for high throughput bacterial cell detection and quantitative analysis. *Nature Microbiology* **1**, 16077 (2016).

175. Brites, D. & Gagneux, S. Co-evolution of Mycobacterium tuberculosis and Homo sapiens. *Immunological Reviews* **264**, 6–24 (2015).

176. Poulton, N. C. & Rock, J. M. Unraveling the mechanisms of intrinsic drug resistance in Mycobacterium tuberculosis. *Front. Cell. Infect. Microbiol.* **12**, 997283 (2022).

177. Addington, W. W. The treatment of pulmonary tuberculosis. Current options. *Arch Intern Med* **139**, 1391–1395 (1979).

178. Batt, S. M., Minnikin, D. E. & Besra, G. S. The thick waxy coat of mycobacteria, a protective layer against antibiotics and the host's immune system. *Biochemical Journal* **477**, 1983–2006 (2020).

179. ABRAHAMS, K. A. & BESRA, G. S. Mycobacterial cell wall biosynthesis: a multifaceted antibiotic target. *Parasitology* **145**, 116–133 (2018).

180. Egan, A. J. F., Errington, J. & Vollmer, W. Regulation of peptidoglycan synthesis and remodelling. *Nat Rev Microbiol* (2020) doi:10.1038/s41579-020-0366-3.

181. FEBS Letters - July 01 1969 - Adam - L acide N-glycolyl-muramique constituant des parois de Mycobacterium smegmatis .pdf.

182. Petit, J. F., Adam, A., Wietzerbin-Falszpan, J., Lederer, E. & Ghuysen, J. M. Chemical structure of the cell wall of Mycobacterium smegmatis. I — Isolation and partial characterization of the peptidoglycan. *Biochemical and Biophysical Research Communications* **35**, 478–485 (1969).

183. Lederer, E., Adam, A., Ciorbaru, R., Petit, J.-F. & Wietzerbin, J. Cell walls of mycobacteria and related organisms; Chemistry and immunostimulant properties. *Mol Cell Biochem* **7**, 87–104 (1975).

184. Jacobo-Delgado, Y. M., Rodríguez-Carlos, A., Serrano, C. J. & Rivas-Santiago, B. Mycobacterium tuberculosis cell-wall and antimicrobial peptides: a mission impossible? *Front. Immunol.* **14**, (2023).

185. Alderwick, L. J., Harrison, J., Lloyd, G. S. & Birch, H. L. The Mycobacterial Cell Wall—Peptidoglycan and Arabinogalactan. *Cold Spring Harb Perspect Med* **5**, (2015).

186. Justen, A. M. *et al.* Polysaccharide length affects mycobacterial cell shape and antibiotic susceptibility. *Sci. Adv.* **6**, eaba4015 (2020).

187. Brown, E. D., Vivas, E. I., Walsh, C. T. & Kolter, R. MurA (MurZ), the enzyme that catalyzes the first committed step in peptidoglycan biosynthesis, is essential in Escherichia coli. *J Bacteriol* **177**, 4194–4197 (1995).

188. Funes Chabán, M. *et al.* Inhibition of MurA Enzyme from Escherichia coli and Staphylococcus aureus by Diterpenes from Lepechinia meyenii and Their Synthetic Analogs. *Antibiotics* **10**, 1535 (2021).

189. Xu, L. *et al.* Characterization of mycobacterial UDP-N-acetylglucosamine enolpyruvyle transferase (MurA). *Research in Microbiology* **165**, 91–101 (2014).

190. Salton, M. R. J. & Kim, K.-S. Structure. in *Medical Microbiology* (ed. Baron, S.) (University of Texas Medical Branch at Galveston, Galveston (TX), 1996).

191. Blake, K. L. *et al.* The nature of *Staphylococcus aureus* MurA and MurZ and approaches for detection of peptidoglycan biosynthesis inhibitors. *Molecular Microbiology* **72**, 335–343 (2009).

192. De Smet, K. A. L., Kempsell, K. E., Gallagher, A., Duncan, K. & Young, D. B. Alteration of a single amino acid residue reverses fosfomycin resistance of recombinant MurA from Mycobacterium tuberculosisThe EMBL accession number for the sequence in this paper is X96711. *Microbiology* **145**, 3177–3184 (1999).

193. Wamp, S. *et al.* PrkA controls peptidoglycan biosynthesis through the essential phosphorylation of ReoM. *eLife* **9**, e56048 (2020).

194. Kock, H., Gerth, U. & Hecker, M. MurAA, catalysing the first committed step in peptidoglycan biosynthesis, is a target of Clp-dependent proteolysis in Bacillus subtilis. *Molecular Microbiology* **51**, 1087–1102 (2004).

195. Boutte, C. C. *et al.* A cytoplasmic peptidoglycan amidase homologue controls mycobacterial cell wall synthesis. *eLife* **5**, e14590 (2016).

196. Jumper, J. *et al.* Highly accurate protein structure prediction with AlphaFold. *Nature* (2021) doi:10.1038/s41586-021-03819-2.

197. García-Heredia, A. *et al.* Peptidoglycan precursor synthesis along the sidewall of pole-growing mycobacteria. *eLife* **7**, (2018).

198. Spassov, D. S., Atanasova, M. & Doytchinova, I. A role of salt bridges in mediating drug potency: A lesson from the N-myristoyltransferase inhibitors. *Front. Mol. Biosci.* **9**, 1066029 (2023).